Magnetic resonance imaging perfusion is associated with disease severity and activity in multiple sclerosis

Piotr Sowa (1, 2), Gro Owren Nygaard (3), Atle Bjørnerud (4, 5), Elisabeth Gulowsen Celius (3, 6), Hanne Finstad Harbo (2, 3), Mona Kristiansen Beyer (1, 7)

(1) Department of Radiology and Nuclear Medicine, Oslo University Hospital, Oslo, Norway
(2) Institute of Clinical Medicine, Faculty of Medicine, University of Oslo, Oslo, Norway
(3) Department of Neurology, Oslo University Hospital, Oslo, Norway
(4) Intervention Center, Oslo University Hospital, Oslo, Norway
(5) Department of Physics, University of Oslo, Oslo, Norway
(6) Institute of Health and Society, Faculty of Medicine, University of Oslo, Oslo, Norway
(7) Department of Life Sciences and Health, Oslo and Akershus University College of Applied Sciences, Oslo, Norway

ABSTRACT

Purpose

The utility of perfusion weighted imaging in multiple sclerosis (MS) is not well investigated. The purpose of this study was to compare baseline normalized perfusion measures in subgroups of newly diagnosed MS patients. We wanted to test the hypothesis that this method can differentiate between groups defined according to disease severity and disease activity at one year follow-up.

Methods

Baseline magnetic resonance imaging (MRI) including a dynamic susceptibility contrast perfusion sequence was performed on a 1.5 Tesla scanner in 66 patients newly diagnosed with relapsing-remitting MS. From the baseline MRI, cerebral blood flow (CBF), cerebral blood volume (CBV) and mean transit time (MTT) maps were generated. Normalized (n) perfusion values were calculated by dividing each perfusion parameter obtained in white matter lesions by the same parameter obtained in normal appearing white matter. Neurological examination was performed at baseline and at follow-up approximately one year later to establish the multiple sclerosis severity score (MSSS) and evidence of disease activity (EDA).

Results

Baseline nMTT was lower in patients with MSSS>3.79 (p=0.016), in patients with EDA (p=0.041) and in patients with both MSSS>3.79 and EDA (p=0.032) at one-year follow-up. Baseline nCBF and nCBV did not differ between these groups.

Conclusions

Lower baseline nMTT was associated with higher disease severity and with presence of disease activity one year later in newly diagnosed MS patients. Further longitudinal studies are needed to confirm whether baseline normalized perfusion measures can differentiate between disease severity and disease activity subgroups over time.

Keywords

Disease activity, Disease severity, Magnetic resonance imaging, Mean transit time, Multiple sclerosis, Perfusion weighted imaging

Abbreviations

CBF = cerebral blood flow; CBV = cerebral blood volume; DMT = disease modifying treatment; EDA = evidence of disease activity; EDSS = expanded disability status scale; MRI = magnetic resonance imaging; MS = multiple sclerosis; MSSS = multiple sclerosis severity score; MTT = mean transit time; n = normalized; NAWM = normal appearing white matter; NEDA = no evidence of disease activity; PVE = partial volume effect; PWI = perfusion weighted imaging; WML = white matter lesions

1. INTRODUCTION

Multiple sclerosis (MS) is an important cause of neurological disability in young adults [1]. The disease varies in terms of severity, and both disease progression and disease activity are difficult to predict at onset [2-5]. Imaging biomarkers that could help in early identification of patients at risk of developing a severe disease course would be a useful tool in clinical management. There have been several attempts to grade disease severity in MS and to identify prognostic parameters for benign and severe disease course, including volumetric measures

[6-10]. To date, no such parameters have been validated. To assess disease severity in MS at a single time point the MS severity score (MSSS) can be used. MSSS describes disease severity as neurological disability in relation to disease duration, and has been proven useful for comparing groups of patients [11]. Disease activity can be assessed using the concept of evidence of disease activity (EDA), based on a composite of clinical and radiological measures. The concept was recently introduced in clinical trials where the absence of EDA – no evidence of disease activity (NEDA), was used as an outcome measure in evaluation of disease modifying treatments (DMT) [12-14].

Magnetic resonance imaging (MRI) is an important tool in diagnosis and follow-up of MS patients [15-17]. Furthermore, advanced MRI has shown promising results in establishing prognosis and in disease monitoring in MS, but it is still not well explored and a need for new MRI markers has been highlighted [10]. One advanced MRI technique is dynamic susceptibility contrast perfusion weighted imaging (PWI) that enables measurement of cerebral blood flow (CBF), cerebral blood volume (CBV) and mean transit time (MTT) in brain tissue [18]. Due to known large technical and biological variations in these perfusion measures only normalized perfusion values can reliably be compared across individuals [19], calculated as the ratio of a perfusion measure from two different brain regions in the same subject. Such normalization has been extensively used in neurooncology [20, 21] and cerebral ischemic disease [22], while in MS it has been used e.g. for assessment of perfusion in lesions normalized to contralateral NAWM [23] or for analyzing the association between clinical data and perfusion in different brain regions normalized to hippocampi [24]. There is some literature describing PWI findings in relation to clinical data in patients with MS [24-27] but, to our knowledge, there are no previous reports exploring normalized perfusion measures in relation to disease severity and activity in MS.

This study is based on perfusion data from our previous baseline study [28] and on clinical data from approximately one-year follow-up [29]. We aimed to investigate whether there are differences in normalized perfusion measures between clinical subgroups of newly diagnosed MS patients, defined according to disease severity and disease activity. We hypothesized that patients with higher severity (higher MSSS scores), with active disease (presence of EDA) and with both higher severity and active disease one year later differ in their baseline normalized perfusion measures from patients with a more benign disease course.

2. MATERIALS AND METHODS

2.1 Subjects

Sixty-six patients newly diagnosed with relapsing-remitting (RR) MS according to the revised 2010 McDonald criteria [17] were prospectively enrolled in this study. The patients were diagnosed with MS between January 2009 and October 2012, and recruited from an on-going longitudinal study at our institution [29]. All patients underwent a detailed neurological examination at baseline within 14.4 ± 9.6 months (range 1–34) from diagnosis. The baseline MRI scan was acquired within a week from the baseline neurological examination. The follow-up neurological examination and the follow-up MRI scan were repeated approximately one year later (on average 14 ± 1.7 months). The inclusion criteria at baseline were: age 18–50 years, no more than three years since MS diagnosis, at least six weeks since the last relapse or steroid treatment, no prior neurological, neurovascular or psychiatric disease, no substantial head injury or drug abuse. The exclusion criteria were: pregnancy or breastfeeding, previous adverse reaction to gadolinium injection and inadequate image quality on MRI scans. The following demographical and clinical measures were obtained in all patients at baseline: age, sex, age at disease onset, time since diagnosis, disease duration, neurological disability as measured by expanded disability status scale (EDSS) [30], number of relapses and use of DMT. MSSS was calculated based on EDSS and disease duration. At baseline, 68% of the patients received first-line DMT, 14 % received second line DMT and 18% no DMT. At follow-up the EDSS was reassessed, the MSSS was calculated, the number of new relapses was recorded and the EDA/NEDA status was determined based on the clinical and radiological progression as previously published [29]. The clinical data could not be obtained in one patient at follow-up. The characteristics of the patient cohort are presented in table 1A.

Table 1. Characteristics of the patient cohort[a], n=66

A. Demographic and clinical characteristics	
Age at baseline, years	34.9 ± 7.2
Female:male ratio	2:1
Age at disease onset, years	32.6 ± 6.7
Time since diagnosis at baseline, months	14.4 ± 9.6
Disease duration at baseline, months	21 (10 – 33)
Time between baseline and follow-up, months	14.0 ± 1.7

Neurological disability by EDSS at follow-up (n=65)	2.0 (1.5 – 2.5)
Disease severity by MSSS at follow-up (n=65)	4.22 ± 1.99
Nr of patients with EDA at follow-up (n=65)	30 (46%)
Patients by disease modifying treatment[b]	
no treatment	12 (18%)
first line treatment	45 (68%)
second line treatment	9 (14%)
B. Imaging characteristics	
Normalized perfusion measures	
nCBF[c]	0.82 ± 0.20
nCBV[c]	1.02 ± 0.30
nMTT[c]	1.27 ± 0.15
Intracranial volume, ml	1445 ± 123
Brain volume[d]	0.81 ± 0.02
Grey matter volume[d]	0.42 ± 0.02
White matter volume[d]	0.38 ± 0.01
WML volume (lesion load), ml	5.3 (2.9 – 7.0)
fraction (%) of white matter volume	0.99 ± 0.53
fraction (%) of intracranial volume	0.38 ± 0.20
Number of WML[e] per patient	20.4 ± 13.7
total number of WML in whole cohort	1347
Contrast enhancing WML	
number of patients with enhancing WML	7 (11%)
number of enhancing WML per patient	1 ± 0
total number of enhancing WML in cohort	7 (0.05%)

EDA: Evidence of disease activity; EDSS: expanded disability status scale; MRI: magnetic resonance imaging; MS: multiple sclerosis; MSSS: multiple sclerosis severity scale; nCBF: normalized cerebral blood flow; nCBV: normalized cerebral blood volume; nMTT: normalized mean transit time; WML: white matter lesions.

[a] Data are *n* (%), mean ± standard deviation, or median (interquartile range).

[b] Disease modifying treatment: first line: interferon, glatiramer acetate, teriflunomide, dimethylfumarate; second line: natalizumab, fingolimod, alemtuzumab.

[c] Normalized perfusion measures calculated as perfusion parameters obtained in WML divided by the same parameters obtained in normal appearing white matter.

[d] Normalized to intracranial volume.

[e] Based on manually corrected WML mask co-registered to perfusion maps.

2.2 Image acquisition

MRI scanning was performed as baseline on the same 1.5 Tesla scanner (Avanto, Siemens Medical, Erlangen, Germany) equipped with a 12-channel head coil. The following sequences were acquired:

(a) Sagittal 3D T1 MPRAGE (FOV: 240 x 240 mm; slice thickness: 1.2 mm; voxel size: 1.3 x 1.3 x 1.2 mm; TR: 2400 ms; TE: 3.61 ms; TI: 1000 ms; flip angle: 8°;
(b) Pre-contrast sagittal 3D FLAIR (FOV: 260 x 260 mm; slice thickness: 1 mm; voxel size: 1 x 1 x 1 mm; TR: 6000 ms; TE: 333 ms; TI: 2200 ms;
(c) Dynamic susceptibility contrast perfusion sequence (19 axial slices; FOV: 230 x 230 mm; slice thickness: 5 mm; voxel size: 1.8 x 1.8 x 5 mm; TR: 1400 ms; TE: 30 ms; flip angle: 90°). I.v. contrast agent (Dotarem, Laboratoire Guerbet, Paris, France) was administered at a dose 0.2 ml/kg and injection rate 5 ml/sec.;
(d) Post-contrast T1 MPRAGE, with parameters identical to those of pre-contrast 3D T1, acquired approximately 7 minutes after contrast agent injection following the PWI acquisition.

2.3 Image processing

Details concerning image processing are given in a previous perfusion study at our institution that used the same patient material [28]. The perfusion data were processed with the nordicICE software package (www.nordicneurolab.com), resulting in CBF, CBV and MTT perfusion parametric maps (figure 1). A population based average arterial input function was used in the perfusion analysis. Correction for partial volume effects (PVE) was not specifically performed due to lack of established methods for this purpose. Proper PVE correction would require knowledge of the point spread function of the perfusion sequence [31], which is not easily obtainable for echo planar imaging sequences. We attempted to reduce PVE by down-sampling the high-resolution lesion mask to perfusion space, thereby avoiding any detrimental re-slicing of the low-resolution perfusion images. In the perfusion analysis, the parameters were adjusted to minimize the influence of the residual leakage. Leakage correction was performed using an established algorithm [32]. The algorithm uses linear fitting to estimate the T1 contamination caused by contrast agent extravasation, and by removing the leakage term it allows generation of corrected perfusion maps.

Figure 1. Typical perfusion maps in a sample patient.

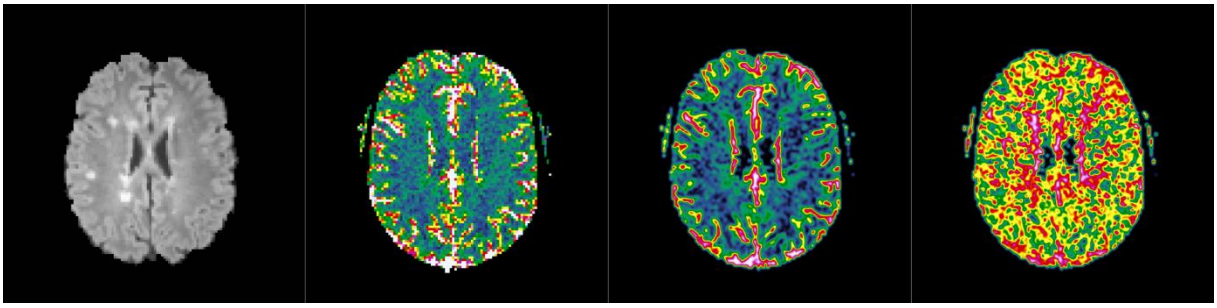

From the left: co-registered FLAIR series and CBF, CBV and MTT maps.

FLAIR: fluid-attenuated inversion recovery; CBF: cerebral blood flow, CBV: cerebral blood volume; MTT: mean transit time.

Binary masks of WM and GM were created from the volumetric T1 series using the Matlab-based Statistical Parametric Mapping toolbox (SPM8; http://www.fil.ion.ucl.ac.uk/spm). Volumetric measures and white matter lesions (WML) masks were generated automatically from the 3D T1 and FLAIR series using the CASCADE software (ki.se/en/nvs/cascade, Karolinska Institute, Stockholm, Sweden) [33]. The volumetric measures were normalized to intracranial volume. The structural series and the binary masks were co-registered to the perfusion maps using SPM8. The co-registered WML masks were visually inspected and edited in nordicICE software by a neuroradiologist to control for errors in the automatic lesion detection. The editing was performed by adding the automatically generated lesion segments as overlays on anatomical FLAIR series, which allowed adding and removing pixels from the WML mask. This correction provided quality control for the final WML masks. Dice similarity coefficient was calculated for the original and the edited WML masks. Region-of-interest analysis was performed to extract perfusion parameters corresponding to the WML and NAWM masks. Normalized (n) perfusion measures were calculated by dividing each perfusion parameter obtained from the whole volume of WML by the same parameter obtained from the whole volume of NAWM. As a result, nCBF, nCBV and nMTT values were calculated for each patient. Normalization to the whole NAWM was chosen due to easy reproducibility and availability of whole WM segmentation methods today, and because previous reports showed that changes in NAWM in MS are general and found in both infra- and supratentorial WM with diffusion tensor imaging [34]. Figure 2 shows WML and NAWM masks overlaid on a MTT perfusion map in a sample patient. In addition, the co-registered WML masks were post-processed using in-house software developed in Matlab R2012a (MathWorks, Natick, MA, USA) to obtain lesion count.

Figure 2. FLAIR series, WM and WML masks and MTT perfusion map in a patient.

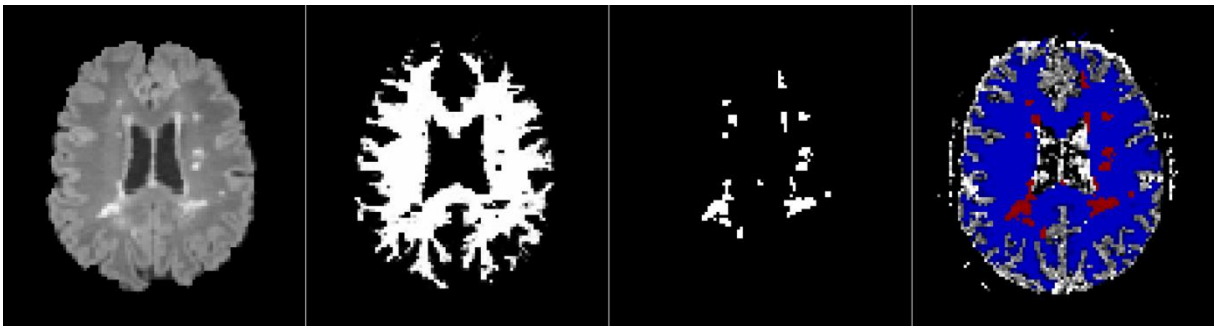

Normalized perfusion measures were calculated by dividing each perfusion parameter obtained in WML (red) by the same parameter obtained in NAWM (blue), using WM and WML masks. Here we see from the left: FLAIR series, WM mask, WML mask, and MTT perfusion map with overlaid WM and WML masks. Different patient than in figure 1.

FLAIR: fluid-attenuated inversion recovery; MTT: mean transit time; NAWM: normal appearing white matter; WM: white matter; WML: white matter lesions

There were only seven contrast-enhancing lesions in our material (one lesion each in seven patients), probably due to the fact that the patients were clinically stable when they came for scanning. In our study we wanted to focus on perfusion properties of the whole volume of lesions, but a separate analysis of the contrast enhancing lesions was performed by us previously [28]. The analysis showed no difference in perfusion parameters between the enhancing and the non-enhancing lesions (p=0.414, p=0.904 and p=0.332 for CBV, CBF and MTT, respectively). For this reason all lesions were included in the final analysis.

2.4 Statistical analysis

The Statistical Package for the Social Sciences software (SPSS v22, IBM, Chicago IL, USA) was used for all statistical analyses. Since the tested normalized perfusion parameters and volumetric measures were normally distributed in Kolmogorov-Smirnov normality test, the parametric one-way between-group analysis of covariance (ANCOVA) test was used for group analysis. Since we previously have shown that the EDA patients included in this study cohort used more first line treatment and less second line treatment than NEDA patients [29], all the group comparisons were performed with disease modifying treatment (DMT) as covariate, to control for possible influence of DMT on the results. Analyses of volumetric parameters were controlled for DMT and for age. All reported *p*-values are two-sided and the significance level was set to 0.05.

3. RESULTS

3.1 Clinical characteristics

Mean age of the patients at baseline was 34.9 ± 7.2 years, female: male ratio was 2:1, mean age at disease onset was 32.6 ± 6.7 years, median disease duration to baseline MRI was 21 months (range 3 – 128) and mean time from diagnosis to baseline MRI was 14.4 ± 9.6 months (Table 1A). MSSS was 4.22 ± 1.99 (n=65) at follow-up. The patients were divided in clinical groups according to disease severity measured by MSSS and according to EDA/NEDA status at follow-up. EDA status was found in 30 patients (46%) patients.

3.2 Imaging findings

The imaging characteristics and volumetric measures are shown in details in table 1B. Mean nMTT was 1.27 ± 0.15. Mean brain volume normalized to intracranial volume was 0.81 ± 0.20. Mean lesion count was 20 ± 14 per patient. Contrast enhancing lesions were observed in 7 patients only (one lesion in each patient), representing 0.5% of all 1347 lesions detected. Median total pixel number of the automatically generated WML mask (registered to perfusion maps) was 323 (range 128 – 1178), median total pixel number of the edited WML mask was 186 (range 24 – 1319) and mean Dice similarity coefficient between the masks was 0.51 ± 0.24. Median absolute MTT values are given in Supplementary table 1.

3.3 Group comparisons

3.3.1 Demographical and clinical characteristics of the groups

The definitions of the groups are described in details below in each comparison. Proportion of females was different in NEDA group compared to EDA group and different in group with MSSS$\leq$3.79 and NEDA compared to group with MSSS>3.79 and EDA. Mean age was different in group with MSSS$\leq$3.79 compared to group with MSSS>3.79 (table 2).

Table 2. Baseline characteristics of the groups, n=65.

	Groups defined according to					
	Disease severity		Disease activity		Disease severity & activity	
	MSSS≤3.79 n=29	MSSS>3.79 n=36	NEDA n=35	EDA n=30	MSSS≤3.79 & NEDA n=44	MSSS>3.79 & EDA n=21
Female	23 (79%)	22 (61%)	31 (89%)[a]	14 (47%)[a]	36 (81%)[b]	9 (43%)[b]
Age, years	32.6 ± 6.5[c]	36.6 ± 6.9[c]	35.3 ± 7.5	34 ± 6.4	34.3 ± 7.5	35.6 ± 5.7
Disease duration, years	1.9 (1.2–4)	1.4 (0.8–2.6)	1.9 (1.3–2.8)	1.2 (0.7–2.5)	1.9 (1.1–3)	1.1 (0.8–2.2)

EDA: evidence of disease activity; MSSS: multiple sclerosis severity score; NEDA: no evidence of disease activity.

Data are *n* (%), mean ± standard deviation, or median (interquartile range).

p-values < 0.05 from $\chi 2$ –tests, independent samples t-tests or Mann-Whitney U tests (as appropriate) are indicated as follows:

[a] Proportion of females was different in NEDA group compared to EDA group;

[b] Proportion of females was different in MSSS≤3.79 and NEDA group compared to MSSS>3.79 and EDA group;

[c] Mean age was different in MSSS≤3.79 group compared to MSSS>3.79 group.

3.3.2 Comparison of groups defined according to disease severity by MSSS at follow-up

Since benign MS is usually defined as EDSS of three or less at least 10 years from disease onset [6-8], we defined the group with higher disease severity as patients with MSSS>3.79 (equivalent to EDSS>3.0 at 10 years of disease duration) and lower severity group as patients with MSSS≤3.79 (equivalent to EDSS≤3.0 at 10 years of disease duration). The nMTT was lower (ANCOVA: p=0.016, F(1,62)=6.12, η^2=0.09) in patients with higher severity (n=36) compared to patients with lower severity (n=29) while nCBF and nCBV did not differ between the groups (table 3A and figure 3A). The baseline whole brain volume was lower (ANCOVA: p=0.043, F(1,62)=4.28, η^2=0.07) in patients with higher severity while GM and WM volumes showed no difference between the MSSS groups (table 4A).

Table 3. Baseline normalized perfusion measures in patient groups defined according to disease severity by MSSS (A), disease activity by EDA/NEDA status (B) and both disease severity and activity (C) at one-year follow-up, n=65.

A. Groups defined according to disease severity by MSSS

	MSSS ≤ 3.79 n=29	MSSS > 3.79 n=36	F, partial η^2	*p*-value[a]
nCBF	0.82 ± 0.18	0.81 ± 0.22	0.02, <0.01	0.896
nCBV	1.05 ± 0.26	1.00 ± 0.33	0.15, <0.01	0.697
nMTT	1.32 ± 0.16	1.23 ± 0.12	6.12, 0.09	**0.016**

B. Groups defined according to disease activity by EDA/NEDA status

	NEDA n=35	EDA n=30	F, partial η^2	*p*-value[a]
nCBF	0.81 ± 0.16	0.82 ± 0.24	<0.01, <0.01	0.965
nCBV	1.03 ± 0.23	1.01 ± 0.36	0.32, <0.01	0.575
nMTT	1.30 ± 0.16	1.23 ± 0.13	4.35, 0.07	**0.041**

C. Groups defined according to both disease severity by MSSS and disease activity by EDA/NEDA status

	MSSS ≤ 3.79 and NEDA n=44	MSSS > 3.79 and EDA n=21	F, partial η^2	*p*-value[a]
nCBF	0.81 ± 0.17	0.82 ± 0.25	<0.01, <0.01	0.953
nCBV	1.03 ± 0.26	1.00 ± 0.37	0.44, <0.01	0.511
nMTT	1.30 ± 0.15	1.21 ± 0.12	4.81, 0.07	**0.032**

EDA: evidence of disease activity; MSSS: multiple sclerosis severity score; nCBF: normalized cerebral blood flow; nCBV: normalized cerebral blood volume; NEDA: no evidence of disease activity; nMTT: normalized mean transit time.

[a] One-way analysis of covariance (ANCOVA), controlled for disease modifying treatment.

Figure 3. Baseline nMTT shown in groups defined according to disease severity by MSSS (A), disease activity by EDA/NEDA status (B) and both disease severity and activity (C), n=65.

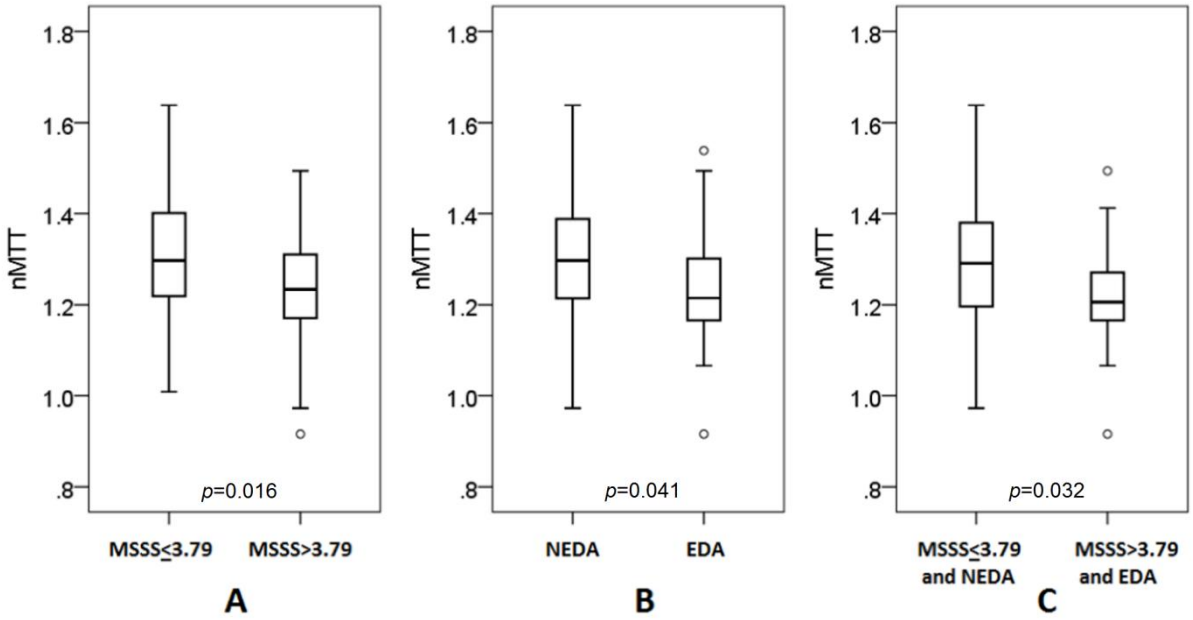

Baseline nMTT was significantly lower (p=0.016) in patients with higher severity of MSSS>3.79 (n=36) compared to patients with lower severity of MSSS≤3.79 (n=29) (A), lower (p=0.041) in patients with EDA (n=30) compared to patients with NEDA (n=35) (B), and lower (p=0.032) in patients with MSSS>3.79 and EDA (n=21) compared to patients with MSSS≤3.79 and NEDA (n=44) (C) at one-year follow-up, controlled for disease modifying treatment. Rings are outliers.

EDA: evidence of disease activity; MSSS: multiple sclerosis severity score; nCBF: normalized cerebral blood flow; nCBV: normalized cerebral blood volume; NEDA: no evidence of disease activity; nMTT: normalized mean transit time.

Table 4. Baseline volumetric data in patient groups defined according to disease severity by MSSS (A), disease activity by EDA/NEDA status (B) and both disease severity and activity (C) at one-year follow-up, n=65.

A. Groups defined according to disease severity by MSSS

	MSSS ≤ 3.79 n=29	MSSS > 3.79 n=36	F, partial η^2	*p*-value[a]
Brain volume[b]	0.82 ± 0.01	0.80 ± 0.02	4.28, 0.07	**0.043**
GM volume[b]	0. 44 ± 0.01	0.43 ± 0.02	1.11, 0.02	0.297
WM volume[b]	0.38 ± 0.01	0.38 ± 0.01	2.83, 0.04	0.097

B. Groups defined according to disease activity by EDA/NEDA status

	NEDA n=35	EDA n=30	F, partial η^2	*p*-value[a]
Brain volume[b]	0.81 ± 0.02	0.81 ± 0.02	1.08, 0.02	0.304
GM volume[b]	0.43 ± 0.02	0.43 ± 0.01	1.49, 0.02	0.226
WM volume[b]	0.38 ± 0.01	0.38 ± 0.01	<0.01, <0.01	0.950

C. Groups defined according to both disease severity by MSSS and disease activity by EDA/NEDA status

	MSSS ≤ 3.79 and NEDA n=44	MSSS > 3.79 and EDA n=21	F, partial η^2	*p*-value[a]
Brain volume[b]	0.81 ± 0.02	0.80 ± 0.02	2.61, 0.04	0.111
GM volume[b]	0.43 ± 0.02	0.43 ± 0.01	1.56, 0.03	0.216
WM volume[b]	0.38 ± 0.01	0.38 ± 0.01	0.57, 0.01	0.455

EDA: evidence of disease activity; GM: grey matter; MSSS: multiple sclerosis severity score; NEDA: no evidence of disease activity; WM: white matter.

[a] One-way analysis of covariance (ANCOVA), controlled for age and disease modifying treatment.

[b] Volumes normalized to intracranial volume.

3.3.3 Comparison of groups defined according to disease activity by EDA/NEDA status.

The participants were grouped according to disease activity as defined by their EDA/NEDA status established at one-year follow-up in a previous clinical study in the same cohort [29] (EDA was defined as a presence of at least one of the following: disability progression, new relapse(s) or radiological progression). Only nMTT differed depending on the EDA/NEDA status: it was lower (ANCOVA: p=0.041, F(1,62)=4.35, η^2=0.07) in the EDA group (n=30) compared to the NEDA group (n=35), while nCBF and nCBV were similar in both groups

(table 3B and figure 3B). The volumetric measurements showed no difference in this comparison (table 4B).

3.3.4 Comparison of groups defined according to disease severity by both MSSS and EDA/NEDA status at follow-up.

In this analysis the patients were divided in two groups according both to their disease severity as measured by MSSS and disease activity defined by EDA/NEDA status. One group was defined as patients with more severe disease course (follow-up MSSS>3.79 and EDA) and the other group as patients with more benign disease course (follow-up MSSS$\leq$3.79 and NEDA). The nMTT was significantly lower in the more severe group (n=21) compared to the more benign group (n=44) after controlling for age and DMT (ANCOVA: p=0.032, $F(1,62)=4.81$, $\eta^2=0.07$) while nCBF and nCBV were similar (table 3C and figure 3C). Hence, nMTT was lower in the less benign group regardless of whether patients were grouped according to MSSS and EDA/NEDA status alone or according to both. The volumetric measurements were similar in this comparison (table 4C).

4. DISCUSSION

In this prospective longitudinal study of newly diagnosed MS patients we found that baseline nMTT was significantly lower in patients with higher disease severity as assessed by MSSS at one-year follow-up. These results suggest that the baseline microvascular properties of MS lesions (related to NAWM) in newly diagnosed MS patients differ with future disease development. Previous studies have revealed heterogeneity of histopathological changes in MS [35-37]. There is ongoing debate about different mechanisms of demyelination [36, 38]. Perivascular T cell infiltration and microglia activation are widespread in many MS patients as well as scattered parenchymal T cell infiltration, also in the chronic disease phase [39]. These findings are also supported in a previous study by Adams et al. [40] who found lymphocytic perivascular infiltration, lesion hypercellularity and macrophage infiltration in MS lesions. In general little is reported about vascular changes associated with MS lesions. Lesions in MS tend to be in perivenular locations [41]. Lassmann et al. [39] reported that disturbances of the microcirculation due to focal edema within inflammatory lesions, inflammatory reaction of the vessel wall resulting in microvascular thrombosis, or endothelial damage by T-lymphocytes are possible mechanisms of demyelination in some patients. An

increased density of microvessels has also been reported by the authors. All these factors may influence perfusion parameters in MS patients. It is therefore plausible that vascular properties of both the WML and NAWM in MS patients can vary across individuals depending on vascular involvement in the pathological changes. In our previous perfusion study we reported reduced perfusion in WML compared to NAWM in MS patients [28]. Thus, lower nMTT in patients with higher disease severity can be interpreted as less reduced (or relatively increased) WML perfusion, which might be caused by different patterns of vascular or perivascular affection in these patients, compared to the patient group with lower disability. Alternatively, this finding could also indicate predominating changes in NAWM (relatively reduced perfusion in NAWM compared to WML).

Furthermore, the nMTT differed significantly between groups defined according to disease activity: it was lower in the EDA group where disease activity was present at one-year follow-up, and in the group defined as patients with both higher disease severity and EDA at follow-up. The fact that higher severity (determined by MSSS) and presence of activity (determined by EDA/NEDA status) were both associated with lower nMTT suggests a similar biological explanation. Interestingly, observed variations in nMTT in our study were not accompanied by a corresponding variation in nCBV or nCBF. This may seem surprising, given that MTT is defined as the ratio CBV/CBF [18]. However, nCBV and nCBF are estimated globally from the ratio of mean values in WML and NAWM whereas MTT is estimated pixel-wise prior to normalization. Hence, nMTT may reveal variations, not reflected in the global nCBV and nCBF measures.

Although only normalized values should be compared between patient groups, we performed additional analysis of absolute MTT values in NAWM and WML between the groups to see which region, WML or NAWM influences the normalized MTT values. This analysis suggested that the nMTT results between MSSS groups are driven mainly by changes in WML ($p=0.048$), and between the EDA/NEDA groups are driven mainly by changes in NAWM ($p=0.025$). The detailed absolute MTT values in the groups are shown in supplementary Table 1. These results should be interpreted with caution as we cannot estimate the influence of physiologically and technically related variations.

The baseline total brain volume was significantly lower in patients with higher severity. This finding is partly in line with previous research reports where whole brain atrophy [42] and

baseline GM volumes [43, 44] were associated with disease severity in MS. No volumetric measures showed significant difference between groups defined according to disease activity (determined by EDA/NEDA status) in our study. In our analyses the nMTT showed more significant results than atrophy measurements in all performed group comparisons.

Our finding of no difference in perfusion measures between enhancing and non-enhancing lesions may seem surprising but it is at least partly supported by a previous study from 2005 [23] where non-enhancing lesions referred to as class "two" were not distinguishable from enhancing lesions in their perfusion properties. In our material, because of a very low number of enhancing lesions (7 of all 1347 lesions detected) the contribution of these lesions to perfusion values would be negligible.

Dice similarity coefficient between the original and the edited WML masks was low (0.51 ± 0.24) which confirms that modification of the original mask (i.e. visual inspection and editing) was necessary.

The strength of the study is that the patients underwent a detailed neurological examination as previously described [29, 45]. The patients were newly diagnosed and are followed longitudinally. The number of participants is relatively large compared to other published perfusion studies in MS which typically included not more than 45 subjects [25-27]. We used a semi-automated image processing method for creating binary masks; this is an advantage as it minimizes the user bias. The perfusion sequence is not time consuming and does not require more intravenous contrast than the standard dose routinely used in MS. Thus this sequence can easily be added to the scanning protocol without increasing scan length with more than two minutes. Our approach in the perfusion analysis (use of normalized perfusion measures, not absolute values) provides reliability for comparisons across subjects, which is also strength of our study.

The main limitation of the study is a short observation time which was 14 months on average. A longer follow-up time is interesting as it would increase the usefulness of the perfusion sequence if it proves to be associated with clinical findings even after 2-3 years or more. Another limitation is that the MRI acquisition was on a 1.5T scanner, this gives a lower signal to noise ratio compared to 3.0 T and may have influenced our results. Our method that required use of lesion segmentation and perfusion analysis may seem time-consuming, but

these techniques are under constant development and even today they are not more complicated than atrophy measurements; moreover, some neuroradiology departments use perfusion techniques routinely, and are familiar with these analyses. Normalization to NAWM in a disease of the whole brain can be questioned, but since the cohort of this study consists of newly diagnosed patients who have not yet reached the progressive phase it can be assumed that pathological changes in NAWM would be subtle in these patients [37]. In addition, a newer perfusion study has suggested normal perfusion in NAWM in MS patients compared to healthy controls [46].

In conclusion, lower baseline nMTT was associated with higher disease severity and with presence of disease activity one year later in newly diagnosed MS patients. This study suggests that MRI perfusion parameters are promising as imaging biomarkers of disease severity and activity in MS, but there is a need for further longitudinal research.

Funding

This study was funded by South-Eastern Norway Regional Health Authority (grant nr 39569). MRI scans and clinical tests were performed within a previous project financed by the same institution (grant nr 2011059).

Conflict of interest

Piotr Sowa received speaker honoraria from Novartis, Genzyme and Biogen.

Gro O. Nygaard received unrestricted research grants from Novartis Norway and from the Odd Fellow's Foundation for Multiple Sclerosis Research.

Atle Bjørnerud is a consultant for NordicNeuroLab AS, Bergen, Norway.

Elisabeth G. Celius received support for travelling and speaker honoraria from Biogen, Genzyme, Merck, Novartis, Sanofi-Aventis and Teva, and received unrestricted research grants from Biogen, Genzyme and Novartis.

Hanne F. Harbo received an unrestricted research grant from Novartis, and support for travelling and speaker honoraria from Biogen, Novartis, Sanofi-Aventis and Teva.

Mona K. Beyer received speaker honoraria from Novartis and Biogen.

Ethical approval

All procedures involving human participants performed in this study were in accordance with the ethical standards of the institutional and national research committee (data inspectorate

representative at the hospital and the Regional Committee for Medical and Health Research Ethics for South-Eastern Norway) and with the 1964 Helsinki declaration and its later amendments.

Informed consent

Written informed consent was obtained from all individual participants included in the study.

Acknowledgments

The authors would like to thank Paulina Due-Tønnessen, Soheil Damangir, Gabriela Spulber and Kyrre Emblem for assistance.

Supplementary Table 1. Baseline absolute MTT values in WML and NAWM in patient groups defined according to disease severity by MSSS (A), disease activity by EDA/NEDA status (B) and both disease severity and activity (C) at one-year follow-up, n=65.

A. Groups defined according to disease severity by MSSS

	MSSS ≤ 3.79 n=29	MSSS > 3.79 n=36	Z, r	*p*-value[a]
MTT in WML[b]	4.60 (2.77-5.87)	4.32 (2.64-8.12)	-1.98,-0.25	**0.048**
MTT in NAWM[b]	3.46 (2.41-4.69)	3.48 (1.98-6.91)	-0.26, -0.03	0.979

B. Groups defined according to disease activity by EDA/NEDA status

	NEDA n=35	EDA n=30	Z, r	*p*-value[a]
MTT in WML[b]	4.28 (2.64-5.87)	4.47 (2.77-8.12)	-1.08,-0.13	0.281
MTT in NAWM[b]	3.32 (1.98-4.24)	3.58 (2.56-6.91)	-2.24,-0.28	**0.025**

C. Groups defined according to both disease severity by MSSS and disease activity by EDA/NEDA status

	MSSS ≤ 3.79 and NEDA n=44	MSSS > 3.79 and EDA n=21	Z, r	*p*-value[a]
MTT in WML[b]	4.30 (2.64-5.87)	4.42 (3.06-8.12)	-0.10,0.01	0.922
MTT in NAWM[b]	3.36 (1.98-4.69)	3.55 (2.71-6.91)	-1.64,0.20	0.101

EDA: evidence of disease activity; MSSS: multiple sclerosis severity score; NAWM: normal appearing white matter; NEDA: no evidence of disease activity; MTT: normalized mean transit time; WML: white matter lesions.

[a] Mann-Whitey *U*-test.

[b] values of MTT are given in seconds, median (range)

References

[1] Nicholas R, Rashid W. Multiple sclerosis. BMJ clinical evidence. 2012;2012.
[2] Rush CA, MacLean HJ, Freedman MS. Aggressive multiple sclerosis: proposed definition and treatment algorithm. Nat Rev Neurol. 2015;11:379-89.
[3] Trojano M, Liguori M, Bosco Zimatore G, Bugarini R, Avolio C, Paolicelli D, et al. Age-related disability in multiple sclerosis. Ann Neurol. 2002;51:475-80.
[4] Confavreux C, Vukusic S. Natural history of multiple sclerosis: a unifying concept. Brain. 2006;129:606-16.
[5] Tremlett H, Zhao Y, Rieckmann P, Hutchinson M. New perspectives in the natural history of multiple sclerosis. Neurology. 2010;74:2004-15.
[6] Ramsaransing GS, De Keyser J. Predictive value of clinical characteristics for 'benign' multiple sclerosis. Eur J Neurol. 2007;14:885-9.
[7] Ramsaransing G, Maurits N, Zwanikken C, De Keyser J. Early prediction of a benign course of multiple sclerosis on clinical grounds: a systematic review. Mult Scler. 2001;7:345-7.
[8] Hawkins SA, McDonnell GV. Benign multiple sclerosis? Clinical course, long term follow up, and assessment of prognostic factors. J Neurol Neurosurg Psychiatry. 1999;67:148-52.
[9] De Stefano N, Airas L, Grigoriadis N, Mattle HP, O'Riordan J, Oreja-Guevara C, et al. Clinical relevance of brain volume measures in multiple sclerosis. CNS drugs. 2014;28:147-56.
[10] Wattjes MP, Rovira A, Miller D, Yousry TA, Sormani MP, de Stefano MP, et al. Evidence-based guidelines: MAGNIMS consensus guidelines on the use of MRI in multiple sclerosis--establishing disease prognosis and monitoring patients. Nat Rev Neurol. 2015;11:597-606.
[11] Roxburgh RH, Seaman SR, Masterman T, Hensiek AE, Sawcer SJ, Vukusic S, et al. Multiple Sclerosis Severity Score: using disability and disease duration to rate disease severity. Neurology. 2005;64:1144-51.
[12] Rotstein DL, Healy BC, Malik MT, Chitnis T, Weiner HL. Evaluation of no evidence of disease activity in a 7-year longitudinal multiple sclerosis cohort. JAMA Neurol. 2015;72:152-8.
[13] Bevan CJ, Cree BA. Disease activity free status: a new end point for a new era in multiple sclerosis clinical research? JAMA Neurol. 2014;71:269-70.
[14] Giovannoni G, Cook S, Rammohan K, Rieckmann P, Sorensen PS, Vermersch P, et al. Sustained disease-activity-free status in patients with relapsing-remitting multiple sclerosis treated with cladribine tablets in the CLARITY study: a post-hoc and subgroup analysis. Lancet Neurol. 2011;10:329-37.
[15] Filippi M, Rocca MA, Ciccarelli O, De Stefano N, Evangelou N, Kappos L, et al. MRI criteria for the diagnosis of multiple sclerosis: MAGNIMS consensus guidelines. Lancet Neurol. 2016;15:292-303.
[16] Rovira A, Wattjes MP, Tintore M, Tur C, Yousry TA, Sormani MP, et al. Evidence-based guidelines: MAGNIMS consensus guidelines on the use of MRI in multiple sclerosis-clinical implementation in the diagnostic process. Nat Rev Neurol. 2015;11:471-82.
[17] Polman CH, Reingold SC, Banwell B, Clanet M, Cohen JA, Filippi M, et al. Diagnostic criteria for multiple sclerosis: 2010 revisions to the McDonald criteria. Ann Neurol. 2011;69:292-302.

[18] Ostergaard L. Principles of cerebral perfusion imaging by bolus tracking. J Magn Reson Imaging. 2005;22:710-7.
[19] Shin W, Horowitz S, Ragin A, Chen Y, Walker M, Carroll TJ. Quantitative cerebral perfusion using dynamic susceptibility contrast MRI: evaluation of reproducibility and age- and gender-dependence with fully automatic image postprocessing algorithm. Magn Reson Med. 2007;58:1232-41.
[20] Emblem KE, Bjornerud A. An automatic procedure for normalization of cerebral blood volume maps in dynamic susceptibility contrast-based glioma imaging. AJNR Am J Neuroradiol. 2009;30:1929-32.
[21] Law M, Young RJ, Babb JS, Peccerelli N, Chheang S, Gruber ML, et al. Gliomas: predicting time to progression or survival with cerebral blood volume measurements at dynamic susceptibility-weighted contrast-enhanced perfusion MR imaging. Radiology. 2008;247:490-8.
[22] Copen WA, Schaefer PW, Wu O. MR perfusion imaging in acute ischemic stroke. Neuroimaging Clin N Am. 2011;21:259-83, x.
[23] Ge Y, Law M, Johnson G, Herbert J, Babb JS, Mannon LJ, et al. Dynamic susceptibility contrast perfusion MR imaging of multiple sclerosis lesions: characterizing hemodynamic impairment and inflammatory activity. AJNR Am J Neuroradiol. 2005;26:1539-47.
[24] Papadaki EZ, Simos PG, Panou T, Mastorodemos VC, Maris TG, Karantanas AH, et al. Hemodynamic evidence linking cognitive deficits in clinically isolated syndrome to regional brain inflammation. Eur J Neurol. 2014;21:499-505.
[25] Papadaki EZ, Simos PG, Mastorodemos VC, Panou T, Maris TG, Karantanas AH, et al. Regional MRI perfusion measures predict motor/executive function in patients with clinically isolated syndrome. Behav Neurol. 2014;2014:252419.
[26] Francis PL, Jakubovic R, O'Connor P, Zhang L, Eilaghi A, Lee L, et al. Robust perfusion deficits in cognitively impaired patients with secondary-progressive multiple sclerosis. AJNR Am J Neuroradiol. 2013;34:62-7.
[27] Inglese M, Adhya S, Johnson G, Babb JS, Miles L, Jaggi H, et al. Perfusion magnetic resonance imaging correlates of neuropsychological impairment in multiple sclerosis. J Cereb Blood Flow Metab. 2008;28:164-71.
[28] Sowa P, Bjornerud A, Nygaard GO, Damangir S, Spulber G, Celius EG, et al. Reduced perfusion in white matter lesions in multiple sclerosis. Eur J Radiol. 2015;84:2605-12.
[29] Nygaard GO, Celius EG, de Rodez Benavent SA, Sowa P, Gustavsen MW, Fjell AM, et al. A Longitudinal Study of Disability, Cognition and Gray Matter Atrophy in Early Multiple Sclerosis Patients According to Evidence of Disease Activity. PLoS One. 2015;10:e0135974.
[30] Kurtzke JF. Rating neurologic impairment in multiple sclerosis: an expanded disability status scale (EDSS). Neurology. 1983;33:1444-52.
[31] Coello C, Willoch F, Selnes P, Gjerstad L, Fladby T, Skretting A. Correction of partial volume effect in (18)F-FDG PET brain studies using coregistered MR volumes: voxel based analysis of tracer uptake in the white matter. Neuroimage. 2013;72:183-92.
[32] Boxerman JL, Schmainda KM, Weisskoff RM. Relative cerebral blood volume maps corrected for contrast agent extravasation significantly correlate with glioma tumor grade, whereas uncorrected maps do not. AJNR Am J Neuroradiol. 2006;27:859-67.
[33] Damangir S, Westman E, Simmons A, Vrenken H, Wahlund L-O, Spulber G. Reproducible segmentation of white matter hyperintensities using a new statistical definition. Magnetic Resonance Materials in Physics, Biology and Medicine. 2016:1-11.
[34] Ciccarelli O, Werring DJ, Wheeler-Kingshott CA, Barker GJ, Parker GJ, Thompson AJ, et al. Investigation of MS normal-appearing brain using diffusion tensor MRI with clinical correlations. Neurology. 2001;56:926-33.

[35] Popescu BF, Pirko I, Lucchinetti CF. Pathology of multiple sclerosis: where do we stand? Continuum (Minneapolis, Minn). 2013;19:901-21.
[36] Stadelmann C, Wegner C, Bruck W. Inflammation, demyelination, and degeneration - recent insights from MS pathology. Biochim Biophys Acta. 2011;1812:275-82.
[37] Kutzelnigg A, Lucchinetti CF, Stadelmann C, Bruck W, Rauschka H, Bergmann M, et al. Cortical demyelination and diffuse white matter injury in multiple sclerosis. Brain. 2005;128:2705-12.
[38] Lassmann H. Axonal injury in multiple sclerosis. J Neurol Neurosurg Psychiatry. 2003;74:695-7.
[39] Lassmann H. Hypoxia-like tissue injury as a component of multiple sclerosis lesions. J Neurol Sci. 2003;206:187-91.
[40] Adams CW, Poston RN, Buk SJ. Pathology, histochemistry and immunocytochemistry of lesions in acute multiple sclerosis. J Neurol Sci. 1989;92:291-306.
[41] Ge Y, Zohrabian VM, Grossman RI. 7T MRI: New Vision of Microvascular Abnormalities in Multiple Sclerosis. Arch Neurol. 2008;65:812-6.
[42] Popescu V, Agosta F, Hulst HE, Sluimer IC, Knol DL, Sormani MP, et al. Brain atrophy and lesion load predict long term disability in multiple sclerosis. J Neurol Neurosurg Psychiatry. 2013;84:1082-91.
[43] Lavorgna L, Bonavita S, Ippolito D, Lanzillo R, Salemi G, Patti F, et al. Clinical and magnetic resonance imaging predictors of disease progression in multiple sclerosis: a nine-year follow-up study. Mult Scler. 2014;20:220-6.
[44] Filippi M, Preziosa P, Copetti M, Riccitelli G, Horsfield MA, Martinelli V, et al. Gray matter damage predicts the accumulation of disability 13 years later in MS. Neurology. 2013;81:1759-67.
[45] Nygaard GO, Walhovd KB, Sowa P, Chepkoech JL, Bjornerud A, Due-Tonnessen P, et al. Cortical thickness and surface area relate to specific symptoms in early relapsing-remitting multiple sclerosis. Mult Scler. 2015;21:402-14.
[46] Ingrisch M, Sourbron S, Herberich S, Schneider MJ, Kumpfel T, Hohlfeld R, et al. Dynamic Contrast-Enhanced Magnetic Resonance Imaging Suggests Normal Perfusion in Normal-Appearing White Matter in Multiple Sclerosis. Invest Radiol. 2016.

Restriction spectrum imaging in multiple sclerosis

Piotr Sowa (1, 2), Hanne F. Harbo (2, 3), Nathan S. White (4), Elisabeth G. Celius (3,5), Hauke Bartsch (4), Pål Berg-Hansen (2,3), Stine M. Moen (3), Lars T. Westlye (6,7), Ole A. Andreassen (7), Anders M. Dale (4,8), Mona K. Beyer (1,9)

(1) Department of Radiology and Nuclear Medicine, Oslo University Hospital, Oslo, Norway
(2) Institute of Clinical Medicine, University of Oslo, Oslo, Norway
(3) Department of Neurology, Oslo University Hospital, Oslo, Norway
(4) Department of Radiology, University of California, San Diego, La Jolla, California, USA
(5) Institute of Health and Society, University of Oslo, Oslo, Norway
(6) Department of Psychology, University of Oslo, Oslo, Norway
(7) NORMENT and K.G. Jebsen Center for Psychosis Research, Division of Mental Health and Addiction, Oslo University Hospital, Oslo, Norway
(8) Department of Neuroscience, University of California, San Diego, La Jolla, California, USA
(9) Department of Life Sciences and Health, Oslo and Akershus University College of Applied Sciences, Oslo, Norway

ABSTRACT

Purpose

Restriction spectrum imaging (RSI) is a newly validated magnetic resonance imaging (MRI) diffusion-based sequence. The aim of the study was to evaluate the association between RSI-derived parameters and neurological disability in multiple sclerosis (MS) patients.

Materials and methods

MRI brain scans including RSI sequence were performed on a 3 Tesla scanner in 80 MS patients (mean age 40.2 years, 63 females) in the period 2013-2014. RSI-derived parameters: fast (fADC) and slow apparent diffusion coefficient (sADC), fractional anisotropy (FA), restricted fractional anisotropy (rFA), neurite density (ND), cellularity, extracellular water fraction (EWF) and free water fraction (FWF) were extracted from the whole volume of white matter lesions (WML) and from normal appearing white matter (NAWM). Patients were grouped according to their expanded disability status scale (EDSS): with minimal, low and

substantial disability (<2.5, 2.5–3 and >3, respectively). Statistical group comparisons and correlation analysis were performed.

Results

In WML, patients with substantial disability had higher fADC (p=0.009), sADC (p=0.005) and FWF (p=0.031), and lower ND (p=0.018) and cellularity (p=0.015) than patients with minimal disability. In NAWM, patients with substantial disability had higher fADC (p=0.021), sADC (p=0.024) and FWF (p=0.033), and lower FA (p=0.027), rFA (p=0.030) and ND (p=0.015) than patients with minimal disability. Parameter that differentiated best between disability subgroups was sADC in WML (p=0.006). Parameter that correlated best with disability was ND in NAWM (ϱ=-0.38, p=0.011).

Conlusion

The sADC in WML differentiated best between disability subgroups, while ND in NAWM showed best correlation with disability. Diffusion parameters derived from RSI are promising imaging biomarkers in MS.

Abbreviations

ADC = apparent diffusion coefficient; DTI = diffusion tensor imaging; EDSS = expanded disability status scale; DWI = diffusion weighted imaging; EWF = extracellular water fraction; FA = fractional anisotropy; fADC = fast apparent diffusion coefficient; GM = grey matter; FWF = free water fraction; MSSS = multiple sclerosis severity score; NAWM = normal appearing white matter; ND = neurite density; rFA = restricted fractional anisotropy; RSI = restriction spectrum imaging; sADC = slow apparent diffusion coefficient; WM = white matter; WML = white matter lesions

1. INTRODUCTION

Multiple sclerosis (MS) is a chronic inflammatory disease of the central nervous system primarily affecting young adults and often resulting in severe neurological disability (1). Even though magnetic resonance imaging (MRI) has an established role in diagnosis and follow-up of MS patients (2-5) there is a need for new imaging biomarkers that could improve the diagnostic and therapeutic precision (3). Diffusion weighted imaging (DWI) is a promising MRI technique in MS. Standard DWI provides the apparent diffusion coefficient (ADC) (6)

while more advanced diffusion techniques have enabled calculation of ADC for the fast and slow diffusion components: fast ADC (fADC) and slow ADC (sADC) (7). Diffusion tensor imaging (DTI) is a multidirectional diffusion MRI (8) that provides fractional anisotropy (FA) informing about the direction of diffusional process.

The results of diffusion studies in MS are not consistent. In a study from 2015 (9) that compared FA, conventional ADC, fADC and sADC in normal appearing white matter (NAWM) between MS patients and healthy controls, only sADC showed significant difference. On the other hand, a study from 2013 (10) reported that both FA and conventional ADC in NAWM differed significantly between MS patients and healthy controls. In this study no correlation between FA or ADC and neurological disability as measured by the expanded disability status scale (EDSS) was detected. Yet another study by Gratsias et al (11) reported a significant correlation between ADC in NAWM and EDSS scores in MS patients. The inconsistent findings can be partly explained by different methodology and different definitions of NAWM across the studies, as well as the non-specific nature of the ADC.

Restriction spectrum imaging (RSI) is a recently validated MRI sequence that is based on measuring water diffusion probed with multiple b-values and various directions (12). This enables a more specific estimation of tissue microstructure compared to “traditional” DWI and DTI techniques (13). The sequence has shown promising results in neuroradiology attempting to improve tumor delineation (14), recover white matter (WM) tracts in peritumoral regions (15) and reflect WM pathology in temporal lobe epilepsy (16) as well as in oncologic imaging of the prostate gland (17-20). In addition to the above-mentioned “traditional” diffusion parameters, RSI also enables calculation of restricted FA (rFA), neurite density (ND), cellularity, extracellular water fraction (EWF) and free water fraction (FWF). This can provide more specific information on white matter lesions (WML) and NAWM, and possibly offer new biomarkers that could be of clinical importance in MS.

The utility of RSI in the work-up of MS patients is unknown. The purpose of this study was to explore the diffusion parameters derived from RSI in WML and NAWM, and to evaluate their association with clinical measures in MS, with focus on neurological disability.

2. MATERIALS AND METHODS

2.1 Ethical approvals

Approval for this study was obtained from the data inspectorate representative at the hospital and from the Regional Committee for Medical and Health Research Ethics for South-Eastern Norway. A signed informed consent was obtained from all study participants.

2.2 Subjects

Eighty MS patients, diagnosed according to the diagnostic criteria revised in 2005 (5), were included in the study. The patients were recruited and referred to MRI by treating neurologists in the period 2013 – 2014 at our institution. Mean age of the patients was 40.2 ± 10.4 years (range 20 – 67), whereof 63 females (mean age 39.6 ± 10.6 years, range 20 – 64) and 17 males (mean age 42.6 ± 9.9 years, range 27 – 67). The inclusion criteria were: age of 18 or more, no prior neurological disease, no contraindication for MRI and no allergy to gadolinium-based contrast media. Since the study was performed in an ambulatory setting we excluded patients completely restricted to bed or wheelchair and unable to move themselves onto the scanner table. Of 109 patients that met the inclusion criteria 29 were excluded, mainly due to technical reasons related to image processing. The flow chart for patient inclusion is shown in Appendix Figure A1.

2.3 Clinical data

Patients were scanned prospectively and the clinical and laboratory data were collected retrospectively from the patients' electronic hospital record: age at disease onset, disease duration, disease subtype, neurological disability assessed with EDSS, and type of disease modifying treatment (see Appendix Text Box 1). EDSS was collected for the date closest to the MRI acquisition. MS disability score (MSSS) (21) was determined, and progression index (defined as EDSS divided by disease duration in years) and age-related disability (defined as EDSS divided by age in years) were calculated. Details concerning demographical, clinical and laboratory data of the patient cohort are shown in Table 1.

Table 1 Demographic and clinical characteristics[a], *n*=80

Age, years	40.2 ± 10.4 (range 20–67)
Female:male ratio	3.7:1
Disease course (patients n=)	
Clinically isolated syndrome	1 (1%)
Relapsing remitting	77 (96%)
Primary progressive	2 (3%)
Age at disease onset, years	27 (25–35)
Disease duration, years	9 (4–14)
EDSS	2.0 (1–2.5)
MSSS	2.32 (0.96–4.26)
Progression index[b]	0.19 (0.10–0.49)
Age-related disability[c]	0.053 ± 0.037
Disease modifying treatment[d] (patients n=)	
no treatment	26 (32%)
first line	23 (29%)
second line	30 (38%)
third line	1 (1%)
Oligoclonal bands in CSF (patients n=)	
yes	72 (90%)
no	7 (9%)
unknown	1 (1%)

CSF: cerebrospinal fluid; EDSS: expanded disability status scale; MSSS: multiple sclerosis severity score.

[a]Data are n (%), mean ± standard deviation, or median (interquartile range).

[b]Progression index defined as EDSS divided by disease duration in years

[c]Age-related disability defined as EDSS divided by age in years

[d]Disease modifying treatment is explained in details in Appendix Text Box 1

2.4 Clinical subgroups

The patients were divided into clinical subgroups based on their neurological disability as measured by EDSS score: group 1 (*n*=28) had minimal disability and EDSS<2.5; group 2 (*n*=41) had low disability and EDSS of 2.5–3 and group 3 (*n*=11) had substantial disability and EDSS>3.

2.5 Image acquisition

All MRI scans were acquired on a 3 Tesla scanner (Signa Optima HDxt, General Electric, Fairfield CT, USA. Seventy-one patients were scanned using an 8-channel head coil and nine patients using a 12-channel head coil, due to technical reasons. All patients were included in final analysis since the distribution of clinical parameters was not significantly different in the two groups. The imaging protocol included the following sequences in all subjects:

(a) Sagittal 3D T1-weighted FSPGR (TE=3-12 ms; TR=7.8 ms; TI=450 ms; FA=12°; FOV=25.6 cm; matrix=256 x 192 mm; slice thickness=1.2 mm);

(b) Sagittal 3D T2-weighted FLAIR CUBE (TE/TR=126.5/6000 ms; TI=1861 ms; FOV=25.6 cm, matrix=256 x 256 mm, slice thickness=1 mm);

(c) Axial single-shot spin-echo diffusion-weighted echo-planar multi-shell RSI sequence (TE=96-289 ms; TR=17 s; FA=90°; FOV=24 cm; matrix=96 x 96 mm; slice thickness=2.5 mm, acquired with b=0, 500, 1500 and 4000 s/mm^2 with 6, 6 and 15 unique gradient directions for each nonzero b-value, respectively), followed by

(d) Post-gadolinium sagittal 3D T1-weighted sequence, with parameters identical to those of pre-gadolinium 3D T1, acquired approximately 5 minutes after i.v. contrast agent injection at a dose of 0.2 ml/kg (Dotarem, Laboratoire Guerbet, Paris, France).

2.6 Image analysis

(a) The preprocessing, RSI processing and co-registration were performed using Matlab software (Matlab Works, Natick MA, USA). Structural scans were corrected for distortions and rigidly registered to each other. The RSI diffusion data were corrected offline for spatial distortions and postprocessed in native space. The derived RSI images were resampled and co-registered to the atlas computed from the structural series. The image data from each participant were visually inspected for quality control. FA was calculated from all b-values: b=0, 500, 1500 and 4000 s/mm^2, fADC was calculated from b=500 data and sADC from the b=4000 data. rFA was calculated from a tensor fit to the restricted water signal derived from the RSI model, with optimal sensitivity to cylindrically restricted diffusion. Also ND, cellularity, EWF and FWF were calculated. Details concerning RSI processing are provided elsewhere (12, 13).

(b) Semi-automated WML segmentation was performed by two radiologists in all 80 subjects using MIPAV software (version 7.2.0, Center for Information Technology, National Institutes of Health, Bethesda MD, USA). The 3D FLAIR series served as a basis for the WML segmentation. As a result, a WML mask representing all lesions was created for each patient. The first author using the MIPAV software performed final visual inspection of the WML mask in each patient.

(c) Freesurfer software (www.freesurfer.net) was used to segment the 3D T1 series to obtain binary masks of WM and grey matter (GM), and the volumetric measures. The masks were visually inspected and corrected for segmentation errors. The WML volume was calculated from the WML mask using NordicICE software (www.nordicneurolab.com). WM volume was calculated using a "lesion filling" approach – first the normal appearing white matter (NAWM) volume was calculated (using WM mask as inclusion mask and WML mask as exclusion mask) and then the volumes of NAWM and WML were summarized.

(d) The diffusion parameters were extracted from the whole volume of WML and from the NAWM. For each patient we calculated fADC, sADC, FA, rFA, ND, cellularity, EWF and FWF mean values in WML and in NAWM. Figure 1 shows schematically WML and WM masks, and the rFA map with and without mask overlays in a sample patient. Matlab software was used for the region of interest analysis.

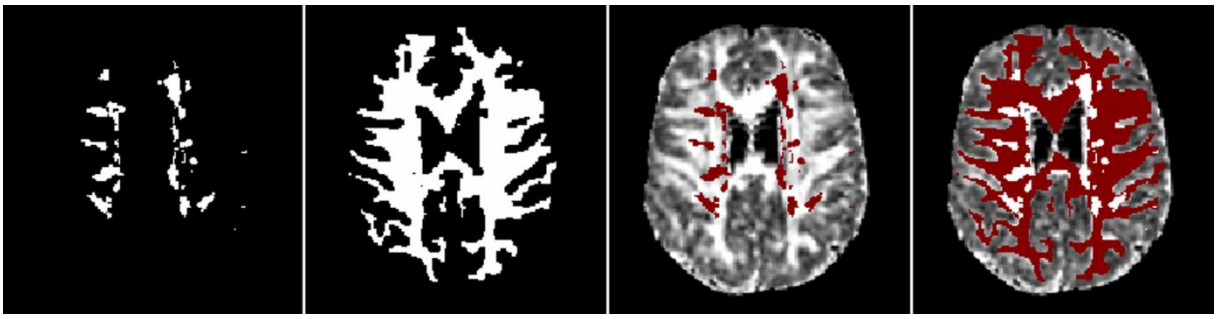

Figure 1 Co-registered binary masks and rFA map in a sample patient

From the left: WML mask, WM mask, rFA map with overlaid WML mask (brown) and rFA map with overlaid WML and WM masks showing NAWM region (brown).

NAWM: normal appearing white matter; rFA: restricted fractional anisotropy; WM: white matter; WML: white matter lesions.

2.7 Statistical analyses

Statistical analyses were performed with the Statistical Package for the Social Sciences software (SPSS v22, IBM, Chicago IL, USA). In addition, the "R" statistical software (v3.1.1, www.r-project.org) was used for the Benjamini-Hochberg false discovery rate method to control for multiple correlations. For group comparisons between two groups the parametric independent samples *t*-test was used when the data were normally distributed; otherwise the non-parametric Mann-Whitney *U* test was used. For group comparisons between three or more groups the parametric one-way analysis of variances (ANOVA) test was used (corrected for multiple comparisons with post-hoc Bonferroni test) when the data were normally distributed; otherwise the non-parametric Kruskal-Wallis *H* test was used (with post-hoc Mann-Whitney *U* test and Bonferroni correction for multiple comparisons). Non-parametric Wilcoxon Signed Rank test was used to test differences in diffusion parameters between WML and NAWM since the data were non-normally distributed in each pair. The Spearman's ϱ (rho) was used for assessing correlations between clinical measures and diffusion parameters as the data were non-normally distributed, otherwise the Pearson's *r* was used for assessing partial correlations (controlled for age). All reported *p*-values are two-sided and $p<0.05$ was defined as level of significance.

3. RESULTS

3.1 Clinical characteristics

Demographic and clinical characteristics are shown in details in Table 1. The median age of disease onset was 27 years, median disease duration was nine years and the median EDSS score was 2.0. Median difference between EDSS date and MRI acquisition date was two months (range 0–8). Seventy-seven patients had a relapsing remitting (RR) form of MS, two had primary progressive (PP) MS and one patient had a clinically isolated syndrome (CIS). 68% of the patients were receiving disease modifying treatment.

3.2 Radiological findings

Detailed radiological characteristics are shown in Table 2a and 2b. Confluent lesions were present in 42 patients (52.5%). In 13 (16%) patients contrast enhancing lesions were observed. Most frequently one or two enhancing lesions per patient were observed, and more

than two enhancing lesions were observed in one patient only. The median WML volume was 4.7 ml (interquartile range 2 – 17.4).

Table 2 Global imaging characteristics[a], *n*=80

a. General characteristics by WML		
Distribution of WML (patients n=)		
- periventricular	77 (96%)	
- juxtacortical	79 (99%)	
- other supratentorial subcortical	77 (96%)	
- infratentorial	40 (50%)	
Confluent WML (patients n=)		
- no confluent lesions	38 (47.5%)	
- beginning confluence	14 (17.5%)	
- definite confluent lesions	28 (35%)	
Patients with enhancing WML	13 (16%)	
b. Volumetric data		
Intracranial volume, ml	1508 ± 154	
Brain volume, ml	1086 ± 115	
White matter volume, ml	464 ± 62	
Grey matter volume, ml	622 ± 60	
Cortical volume, ml	462 ± 48	
WML volume, ml[b]	4.7 (2–17.4)	
c. Diffusion parameters derived from RSI[c]		
	In WML	*In NAWM*
fADC	1.19 ± 0.14	0.92 (0.90–0.95)
sADC	0.57 ± 0.06	0.47 (0.46–0.49)
FA	0.32 ± 0.04	0.35 (0.33–0.36)
rFA	0.70 ± 0.05	0.65 (0.62–0.66)
ND	354 ± 51	441 (423–449)
Cellularity	107 (89–145)	194 (182–206)
EWF	695 ± 28	728 (717–734)
FWF	563 ± 58	415 (406–428)

fADC: fast apparent diffusion coefficient; EWF: extracellular water fraction; FA: fractional anisotropy; FWF: free water fraction; NAWM: normal appearing white matter; ND: neurite density; RSI: restricted spectrum imaging; sADC: slow apparent diffusion coefficient; rFA: restricted fractional anisotropy; WML: white matter lesions

[a]Data are *n* (%), mean ± standard deviation, or median (interquartile range).

[b]WML volume (lesion load) based on semi-automated segmentation on FLAIR series.

[c]Units for diffusion parameters are given in Appendix Table A1.

3.3 Diffusion parameters in WML and NAWM

The fADC, sADC, FA, rFA, ND, cellularity, EWF and FWF parameters are described and explained closer in Appendix Table A1 and their values in WML and NAWM are presented in Table 2c. The fADC is in theory more sensitive to changes in extracellular diffusion compared with sADC, but these parameters should not be simply ascribed to specific microcompartments. The rFA is the FA derived from the restricted signal from cylindrical structures. ND is the signal fraction of cylindrically restricted water, reflecting the density of neurites in tissue. The EWF represents the signal fraction of water that is hindered due to tortuous geometry of the extracellular space while the FWF is the signal fraction of freely diffusing water. All the tested diffusion parameters differed significantly between WML and NAWM ($p<0.001$ for all pairwise comparisons): fADC, sADC, rFA, and FWF were higher in WML than in NAWM, while FA, ND, cellularity and EWF were lower in WML than in NAWM.

3.4 Comparison of subgroups defined according to neurological disability measured by EDSS

The clinical and MRI characteristics of each disability subgroup are presented in Table 3 and the differences in diffusion parameters between the subgroups are shown schematically in Figure 2. The diffusion parameter that differentiated best between disability subgroups was sADC in WML (ANOVA: F=5.5, eta-squared=0.13, p=0.006). Briefly, the fADC, sADC, ND and FWF differed significantly between the disability subgroups when obtained both in WML (p=0.011, p=0.006, p=0.023 and p=0.036 respectively) and in NAWM (p=0.013, p=0.027, p=0.008 and p=0.014 respectively). Cellularity differed between the disability subgroups only when obtained in WML (p=0.012) while FA and rFA differed between the subgroups only when obtained in NAWM (p=0.022 and p=0.021 respectively). EWF did not differ between the subgroups neither when obtained in WML nor in NAWM. Post-hoc comparisons indicated the greatest differences between the subgroups with substantial disability and minimal disability: in WML patients with substantial disability had *higher* fADC (p=0.009), sADC (p=0.005) and FWF (p=0.031), and *lower* ND (p=0.018) and cellularity (p=0.015) while in NAWM patients with substantial disability had *higher* fADC (p=0.021), sADC (p=0.024) and FWF (p=0.033), and *lower* FA (p=0.027), rFA (p=0.030) and ND (p=0.015) than patients with minimal disability.

Table 3 Differences between disability subgroups[a], *n*=80

	Neurological disability by EDSS			F, η^2 or H, w^2	*p*-value
	minimal EDSS < 2.5	low EDSS of 2.5 - 3	substantial EDSS > 3		
	n=28	*n*=41	*n*=11		
Characteristics					
Age, years	37.4 ± 8.9	41.2 ± 11.1	43.8 ± 10.2	1.9, 0.05[b]	0.153[b]
Age at disease onset, years	27 (25–31)	29 (26–37.5)	25 (22–35)	3.5, 0.04[c]	0.177[c]
Disease duration, years	7.5 (4–12)	9 (3–15.5)	13 (9–27)	6.5, 0.08[c]	0.038[c]
WML volume, ml	2.7 (1.2–14.1)	4.4 (1.9–15)	19.7 (9.5–31.5)	10.4, 0.13[c]	0.005[c]
Brain volume[d], %	73 ± 5.6	72.4 ± 4.5	68.7 ± 3.4	3.5, 0.08[b]	0.036[b]
Diffusion parameters in WML					
fADC	1.16 ± 0.14	1.18 ± 0.13	1.30 ± 0.19	4.7, 0.10[b]	0.011[b,e]
sADC	0.56 ± 0.06	0.57 ± 0.05	0.62 ± 0.05	5.5, 0.13[b]	0.006[b,f]
FA	0.33 ± 0.05	0.32 ± 0.04	0.30 ± 0.04	2.1, 0.05[b]	0.128[b]
rFA	0.70 ± 0.05	0.69 ± 0.05	0.70 ± 0.04	0.2, 0.01[b]	0.793[b]
ND	368 ± 55	355 ± 47	319 ± 46	4.0, 0.09[b]	0.023[b,g]
Cellularity	125 ± 40	118 ± 37	86 ± 26	8.8, 0.11[c]	0.012[c,h]
EWF	699 ± 27	697 ± 28	677 ± 27	2.8, 0.07[b]	0.070[b]
FWF	548 ± 62	563 ± 54	601 ± 52	3.5, 0.08[b]	0.036[b,i]
Diffusion parameters in NAWM					
fADC	0.92. ± 0.04	0.93 ± 0.04	0.97 ± 0.07	8.7, 0.11[c]	0.013[c,j]
sADC	0.46 ± 0.02	0.47 ± 0.02	0.49 ± 0.02	7.2, 0.09[c]	0.027[c,k]
FA	0.34 ± 0.02	0.34 ± 0.02	0.32 ± 0.03	7.6, 0.10[c]	0.022[c,l]
rFA	0.64 ± 0.02	0.64 ± 0.02	0.62 ± 0.03	7.8, 0.10[c]	0.021[c,m]
ND	440 ± 19	436 ± 18	414 ± 30	9.6, 0.12[c]	0.008[c,n]
Cellularity	200 ± 25	198 ± 30	178 ± 29	5.2, 0.07[c]	0.074[c]
EWF	726 ± 10	724 ± 16	726 ± 18	0.5, 0.01[c]	0.779[c]
FWF	413 ± 20	421 ± 21	439 ± 30	8.6, 0.11[c]	0.014[c,o]

EDSS:expanded disability status scale; EWF: extracellular water fraction; FA: fractional anisotropy; fADC: fast apparent diffusion coefficient; FWF: free water fraction; ND: neurite density; sADC: slow apparent diffusion coefficient; rFA: restricted fractional anisotropy; WML: white matter lesions

[a]Data are mean ± standard deviation, or median (interquartile range)

[b]One way Anova test (normally distributed data), the next to last column shows F and eta-squared

[c]Kruskal-Wallis *H*-test (non-normally distributed data), the next to last column shows H and w-squared

[d]Normalized brain volume (in percent of intracranial volume)

[e]significant difference between group 3 and groups 1 and 2 (p=0.009 and p=0.034 respectively)

[f]significant difference between group 3 and groups 1 and 2 (p=0.005 and p=0.016 respectively)

[g]significant difference between group 3 and group 1 (p=0.018)

[h]significant difference between group 3 and groups 1 and 2 (p=0.015 and p=0.036 respectively)

[i]significant difference between group 3 and group 1(p=0.031)

[j]significant difference between group 3 and group 1 (p=0.021)

[k]significant difference between group 3 and group 1 (p=0.024)

[l]significant difference between group 3 and group 1 (p=0.027)

[m]significant difference between group 3 and groups 1 and 2 (p=0.030 both)

[n]significant difference between group 3 and groups 1 and 2 (p=0.015 and p=0.036 respectively)

[o]significant difference between group 3 and groups 1 and 2 (p=0.033 and p=0.048 respectively)

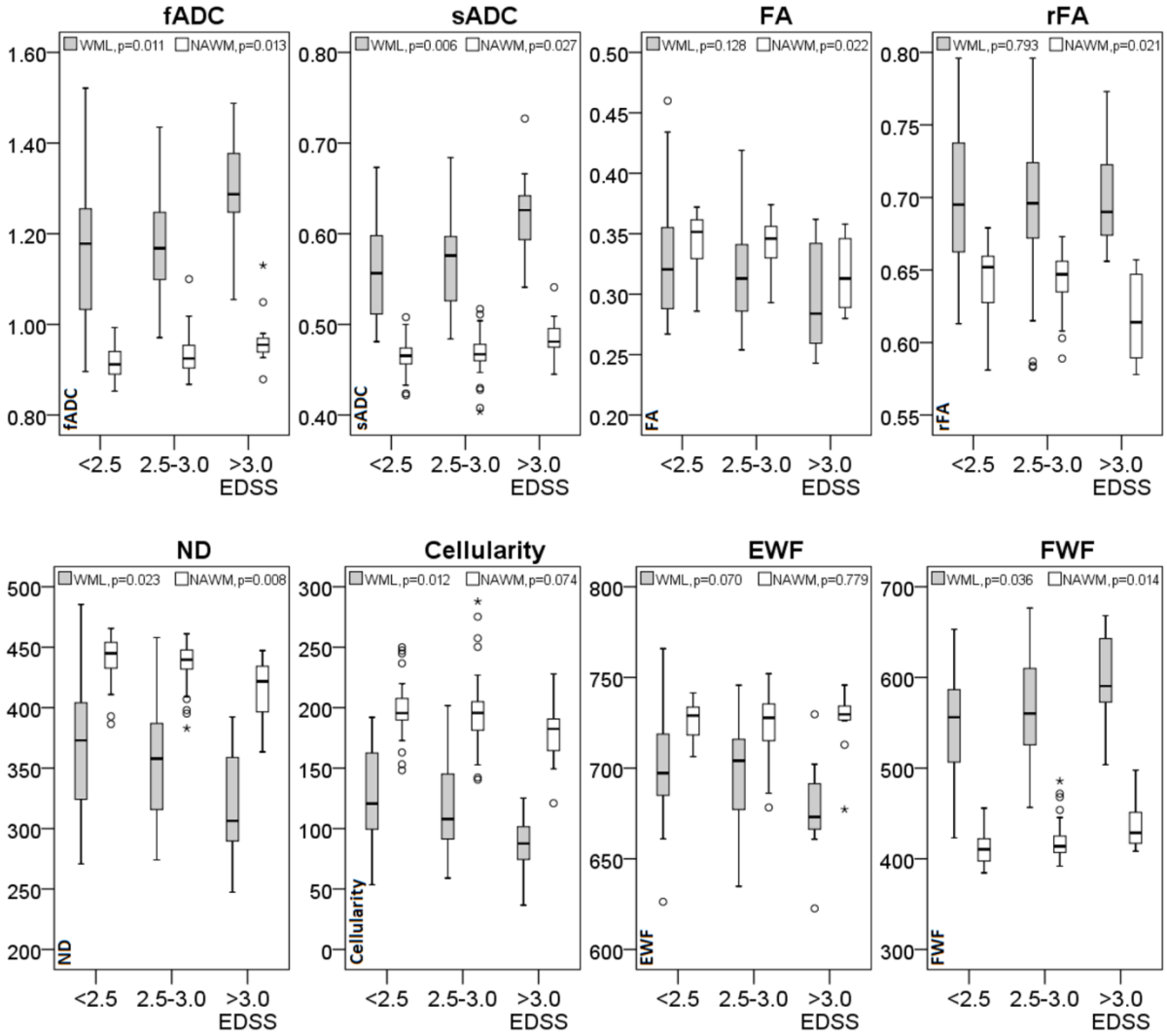

Figure 2 Diffusion parameters in WML and NAWM shown by disability subgroups, *n*=80

The gray bars represent WML, the white bars represent NAWM. The units are explained in Appendix Table A1. Upper row: fADC, sADC, FA and rFA in WML (grey bars) and NAWM (white bars) shown by EDSS subgroups. Lower row: ND, cellularity, EWF and FWF in WML (grey bars) and NAWM (white bars) shown by EDSS subgroups. Subgroups are defined by neurological disability: no or minimal (EDSS<2.5, n= 28), low (EDSS of 2.5 or 3.0, n=41), and substantial (EDSS>3.0, n=11) disability.

EDSS: expanded disability status scale; EWF: extracellular water fraction; fADC: fast apparent diffusion coefficient; FA: fractional anisotropy; FWF: free water fraction; NAWM: normal appearing white matter; ND:

neurite density; rFA: restricted fractional anisotropy; sADC: slow apparent diffusion coefficient; WML: white matter lesions.

3.5 Correlations between clinical data, and volumetric and diffusion parameters

Details concerning correlations between the clinical data and volumetric and diffusion parameters are shown in Table 4. EDSS correlated with brain volume (r=-0.24, *p*=0.049), WM volume (r=-0.28, *p*=0.023) and WML volume (r=0.25, *p*=0.043), controlled for age. Of the diffusion parameters, EDSS correlated with fADC (ϱ=0.35, *p*=0.011), sADC (ϱ=0.32, *p*=0.013), ND (ϱ=-0.30, *p*=0.017), cellularity (ϱ=-0.29, *p*=0.021), EWF (ϱ=-0.30, *p*=0.017) and FWF (ϱ=0.32, *p*=0.013) in WML, and with fADC (ϱ=0.35, *p*=0.011), FA (ϱ=-0.32, *p*=0.013), rFA (ϱ=-0.29, *p*=0.021), ND (ϱ=-0.38, *p*=0.011) and FWF (ϱ=0.33, *p*=0.011) in NAWM. For correlations with disease duration see Table 4. MSSS, progression index and age-related disability did not correlate with any of the investigated diffusion or volumetric parameters.

Table 4 Correlations between clinical data, and volumetric and diffusion parameters, *n*=80

	EDSS[a]	Disease duration[a]
Volumetric data[b]	r, *p*	r, *p*
Whole brain[c]	-0.24, **0.049**	-0.04, 0.753
White matter[c]	-0.28, **0.023**	-0.03, 0.810
Grey matter[c]	-0.14, 0.269	-0.04, 0.753
Cortex[c]	-0.11, 0.391	-0.06, 0.697
WML volume	0.25, **0.043**	0.42, <**0.001**
- % of white matter volume	0.26, **0.035**	0.41, <**0.001**
- % of intracranial volume	0.25, **0.041**	0.42, <**0.001**
Diffusion parameters in WML	ϱ, *p*	ϱ, *p*
fADC	0.35, **0.011**	0.40, <**0.001**
sADC	0.32, **0.013**	0.28, **0.021**
FA	-0.21, 0.073	-0.11, 0.441
rFA	0.02, 0.877	0.11, 0.441
ND	-0.30, **0.017**	-0.28, **0.021**
Cellularity	-0.29, **0.021**	-0.22, 0.084
EWF	-0.30, **0.017**	-0.44, <**0.001**
FWF	0.32, **0.013**	0.37, **0.003**
Diffusion parameters n NAWM	ϱ, *p*	ϱ, *p*
fADC	0.35, **0.011**	0.32, **0.008**

sADC	0.23, 0.051	0.13, 0.334
FA	-0.32, **0.013**	-0.38, **0.002**
rFA	-0.29, **0.021**	-0.43, **0.001**
ND	-0.38, **0.011**	-0.35, **0.005**
Cellularity	-0.21, 0.073	-0.10, 0.448
EWF	-0.05, 0.665	-0.20, 0.113
FWF	0.33, **0.011**	0.32, **0.008**

EDSS: expanded disability status scale; EWF: extracellular water fraction; fADC: fast apparent diffusion coefficient; FA: fractional anisotropy; FWF: free water fraction; NAWM: normal appearing white matter; ND: neurite density; rFA: restricted fractional anisotropy; r: partial correlation; ϱ (rho): Spearman's correlation; sADC: slow apparent diffusion coefficient; WML: white matter lesions

Multiple sclerosis severity score (MSSS), progression-index and age-related disability did not correlate significantly with any diffusion parameters and are not included in the table.

[a]Controlled for multiple correlations using Benjamini-Hochberg false discovery rate method

[b]Correlations with volumetric data are controlled for age

[c]Normalized to intracranial volume

4. DISCUSSION

The RSI-derived sADC in WML differentiated best between disability subgroups in MS patients and it was higher in patients with higher disability. Increased sADC in WML in these patients may be due to greater exchange of intracellular and extracellular water compartments, possibly caused by demyelination. There is limited literature available on comparisons of diffusion parameters in WML or NAWM between clinical subgroups in MS, or on correlation of these parameters with clinical data. Droogan et al. in a study from 1999 compared average ADC derived from manually segmented lesions and NAWM regions in clinical subgroups of patients stratified by disease course, with a negative result (22). The authors also reported no significant correlation between ADC values in lesions and EDSS, which is in contradiction to our findings that show such a correlation between ADC (both fADC and sADC) in lesions and EDSS. Gratsias et al. in a study from 2015 (11) reported a correlation between ADC in NAWM and EDSS (which is in accordance with our results) and no correlation between FA in NAWM and EDSS (contrary to our results). These differences may be at least partly due to different methodology used in the studies, e.g. different patient cohorts and different definition of NAWM.

ND that represents the volume fraction of cylindrically restricted water and in theory shows the density of axons and dendrites in the brain tissue was the parameter that showed best correlation with disability when obtained in NAWM. This finding in general supports the results published newly by Brownlee et al. in 2016 who reported an association between neurological disability and lower ND values in NAWM obtained with a diffusion technique named “neurite orientation dispersion and density imaging” (NODDI) in relapse-onset MS patients (23).

All diffusion parameters investigated in our study differed significantly in pairwise comparisons between WML and NAWM: fADC, sADC, rFA, and FWF were higher in WML than in NAWM, while FA, ND, cellularity and EWF were lower in WML than in NAWM. These results, considering the “traditional” ADC and FA parameters, are in accordance (despite somewhat different methodology) with previous reports from the above cited studies by Gratsias et al. (11) and Droogan a et al. (22) who reported higher ADC and lower FA in WML compared to segmented NAWM regions. Histopathologically, FA correlates with myelin content and axonal count in NAWM and WML (24), with lower FA indicating reduced myelin content and lower axonal count. No other study on MS is available to compare our findings with results from others regarding the RSI-derived parameters. ND was found lower and FWF was found higher in WML than in NAWM, which can be explained by reduced axonal count in WML compared to NAWM reported in previous pathological studies (24, 25). The rFA values in WML were significantly higher compared to NAWM as against to FA values that were lower in WML. Lower rFA values in NAWM can be caused by the large region of interest leading to partial voluming of gray matter as well as including areas of crossing fibers in the computation. Both of these factors will reduce the mean rFA value in NAWM compared with WML.

Whole brain volume and WM volume normalized to intracranial volume correlated negatively with disability (controlled for age) which supports previous reports: Shiee et al. in a study from 2012 (26) reported an association between lower WM volume and higher disability in MS patients. WML volume showed a moderate positive correlation with disability considering both absolute values and values normalized to WM or intracranial volume; this finding is in accordance with previous publications where disability in MS patients was reported to correlate with absolute WML volume (27) and WML volume normalized to WM (28).

This study has both strengths and limitations. The study group was large (n=80) and consisted of patients in different stages of the disease. The RSI technique that we used is a recently validated MRI method previously not applied in MS, and we used largely unbiased methods of analysis. A small group of experienced neurologists at the university hospital examined all patients. Limitations were having neither healthy controls nor tissue samples available, and also that clinical data were retrospectively collected. So far we do not have longitudinal data from these patients. Thus, better validation of the RSI method in experimental studies is needed.

In conclusion, RSI-derived sADC and ND are promising imaging biomarkers that best discriminated between disability subgroups and best correlated with disability in MS, and may become useful for disease monitoring in MS patients. Contrary to the established DTI sequence, RSI provides more specific diffusion parameters and offers a more detailed method for imaging of brain tissue in MS.

Funding information

This study received funding from South-Eastern Norway Regional Health Authority (project nr 39569). The project was also supported by grants for MRI acquisitions from the Odd Fellow's Foundation for Multiple Sclerosis Research, Norwegian Society of Radiology and Norwegian Research School in Medical Imaging, and by a travel grant from Ullevålfondet (Ullevål Foundation).

Conflicts of interest

Piotr Sowa received speaker's fees from Novartis, Genzyme and Biogen Idec.
Hanne F. Harbo received an unrestricted research grant from Novartis, and travel support and speaker's fees from Biogen Idec, Genzyme, Novartis, Sanofi-Aventis and Teva.
Nathan S. White received a research grant from General Electric Healthcare (GEHC).
Elisabeth G. Celius received travel support and speaker's fees from Biogen Idec, Genzyme, Merck, Novartis, Sanofi-Aventis and Teva, and unrestricted research grants from Biogen Idec, Genzyme and Novartis.
Pål Berg-Hansen received an unrestricted research grant from Novartis, and travel support and speaker's fees from Novartis, UCB and Teva.

Stine M. Moen received unrestricted research grant from Novartis and unrestricted travel grant and speaker's fees from Biogen Idec and Novartis.
Ole A. Andreassen received speaker's fees from Lundbeck, Lilly and Otsuka.
Anders M. Dale is a Founder of and holds equity in CorTechs Labs, Inc., and serves on its Scientific Advisory Board. He is also a member of the Scientific Advisory Board of Human Longevity, Inc. (HLI), and receives research funding from General Electric Healthcare (GEHC). The terms of these arrangements have been reviewed and approved by the University of California, San Diego in accordance with its conflict of interest policies.
Mona K. Beyer received speaker's fees from Novartis and Biogen Idec.
Hauke Bartsch and Lars T. Westlye do not report any conflicts of interest.

Acknowledgements

The authors would like to thank Anne Hilde Farstad, Martina Jonette Lund, Rigmor Lundby, Wibeke Nordhøy, Tomas Sakinis and Niels Petter Sigvartsen for assistance.

APPENDIX

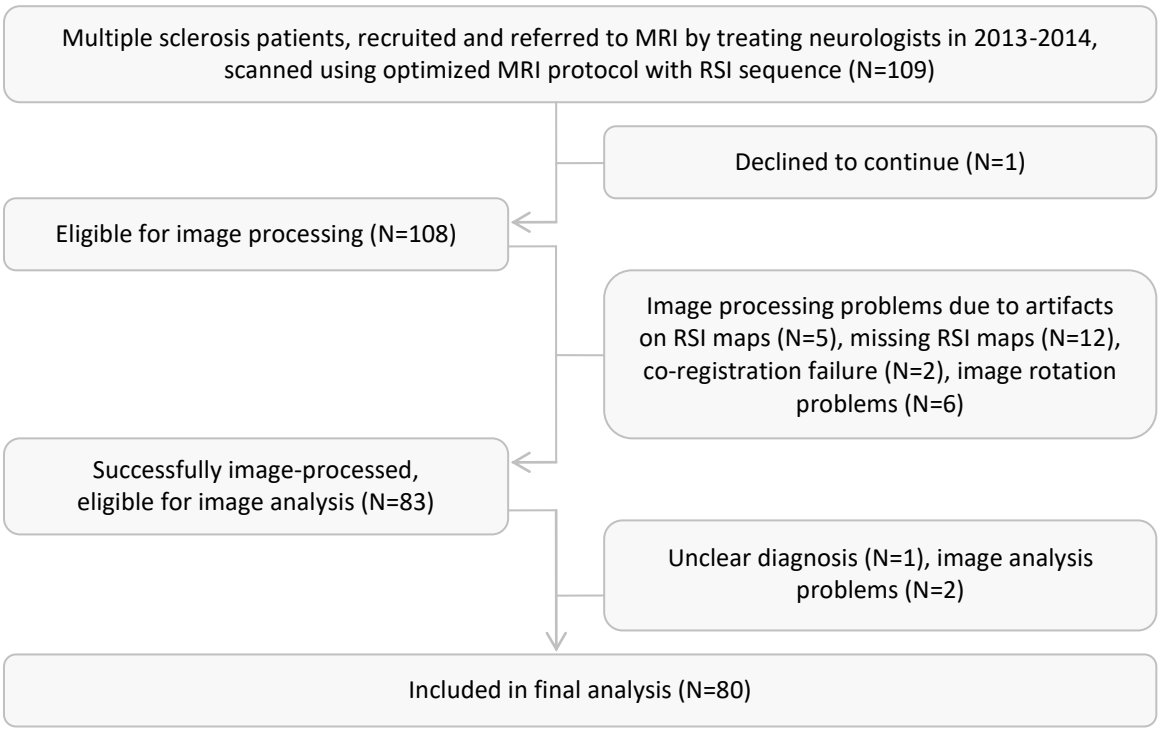

Figure A1 Flow chart for patients' inclusion

Of 109 patients included initially, 80 were included in final analysis.

RSI: Restriction spectrum imaging.

Text Box 1 Disease modifying treatment

Type of disease modifying treatment was defined as first line (interferon, glatiramer acetate, teriflunomide, dimethylfumarate), second line (natalizumab, fingolimod, alemtuzumab) or third line (autologous haematopoietic stem cell transplantation). Due to possible prolonged efficacy of disease modifying treatment after withdrawal, patients who were *not* on treatment at the MRI acquisition date were nonetheless classified as on treatment if the MRI acquisition was performed within 3 months after withdrawal (n=8), or within one year after stem cell transplantation (n=1) or last administration of alemtuzumab (n=3). Immunoglobulin G (IgG) index in cerebrospinal fluid (CSF) and information about the presence of oligoclonal bands in the CSF were also collected.

Table A1 Description of diffusion parameters derived from RSI sequence

Diffusion parameter	Description
Cellularity	Signal fraction from spherically restricted water compartment, i.e. cell bodies. Lower cellularity values mean decreased number of cell bodies, e.g. glial cell bodies in white matter. Unit: 1000*(signal fraction from restricted isotropic compartment), example: 300 means 30% of the total signal stems from this compartment.
EWF	Extracellular water fraction. Represents the signal fraction of water that is hindered due to tortuous geometry of the extracellular space that may be isotropic or anisotropic. It will be reduced if there is a tissue loss or changes in tissue that reduce geometrical complexity and tortuosity. Unit: 1000*(signal fraction from extracellular water compartment).
FA	Fractional anisotropy indicates the degree of anisotropy (or directional dependence); it is given in values between 0 and 1 where 0 means equal diffusion in all directions and 1 means diffusion in one direction only.
fADC	Fast apparent diffusion coefficient. In theory, the fADC measures the effective diffusion coefficient of extracellular water. As such the fADC should be more sensitive to changes in extracellular diffusion (edema or inflammation)

	compared with sADC. However, the fast and slow ADC components are not based on the RSI model, and should not be ascribed to specific microcompartments. Unit: $10^{-3}mm^2/s$.
FWF	Free water fraction. Signal fraction of freely diffusing isotropic water. It will be increased with tissue loss. Unit: 1000*(signal fraction from isotropic free water compartment).
ND	Neurite density. Signal fraction of cylindrically restricted water. Lower ND means reduction of cylindrical structures which in brain tissue is consistent with neurofibers or neurites (axons and dendrites). Unit: 1000*(signal fraction from restricted cylindrical compartment).
rFA	Restricted fractional anisotropy (or tubularity) is the FA derived from the restricted water signal from cylindrical structures, which in theory stems from the intraaxonal and intradendritic (i.e. neurite) compartment. Unit: values between 0 and 1.
sADC	Slow apparent diffusion coefficient. In theory, the sADC measures the effective diffusion coefficient of intracellular water in both cell bodies and neurites. Unit: 10-3mm2/s.

REFERENCES

1. Compston A, Coles A. Multiple sclerosis. Lancet. 2008;372(9648):1502-17. Epub 2008/10/31. doi: 10.1016/s0140-6736(08)61620-7. PubMed PMID: 18970977.

2. Filippi M, Rocca MA, Ciccarelli O, De Stefano N, Evangelou N, Kappos L, et al. MRI criteria for the diagnosis of multiple sclerosis: MAGNIMS consensus guidelines. Lancet Neurol. 2016;15(3):292-303. Epub 2016/01/30. doi: 10.1016/s1474-4422(15)00393-2. PubMed PMID: 26822746; PubMed Central PMCID: PMCPMC4760851.

3. Wattjes MP, Rovira A, Miller D, Yousry TA, Sormani MP, de Stefano MP, et al. Evidence-based guidelines: MAGNIMS consensus guidelines on the use of MRI in multiple sclerosis--establishing disease prognosis and monitoring patients. Nat Rev Neurol. 2015;11(10):597-606. Epub 2015/09/16. doi: 10.1038/nrneurol.2015.157. PubMed PMID: 26369511.

4. Rovira A, Wattjes MP, Tintore M, Tur C, Yousry TA, Sormani MP, et al. Evidence-based guidelines: MAGNIMS consensus guidelines on the use of MRI in multiple sclerosis-clinical implementation in the diagnostic process. Nat Rev Neurol. 2015;11(8):471-82. Epub 2015/07/08. doi: 10.1038/nrneurol.2015.106. PubMed PMID: 26149978.
5. Polman CH, Reingold SC, Banwell B, Clanet M, Cohen JA, Filippi M, et al. Diagnostic criteria for multiple sclerosis: 2010 revisions to the McDonald criteria. Ann Neurol. 2011;69(2):292-302. Epub 2011/03/10. doi: 10.1002/ana.22366. PubMed PMID: 21387374; PubMed Central PMCID: PMCPMC3084507.
6. Schaefer PW, Grant PE, Gonzalez RG. Diffusion-weighted MR imaging of the brain. Radiology. 2000;217(2):331-45. Epub 2000/11/04. doi: 10.1148/radiology.217.2.r00nv24331. PubMed PMID: 11058626.
7. Liu Z, Xiao X. The use of multi b values diffusion-weighted imaging in patients with acute stroke. Neuroradiology. 2013;55(3):371-6. Epub 2013/01/22. doi: 10.1007/s00234-012-1129-2. PubMed PMID: 23334433.
8. Alexander AL, Lee JE, Lazar M, Field AS. Diffusion tensor imaging of the brain. Neurotherapeutics. 2007;4(3):316-29. Epub 2007/06/30. doi: 10.1016/j.nurt.2007.05.011. PubMed PMID: 17599699; PubMed Central PMCID: PMCPMC2041910.
9. Tachibana Y, Obata T, Yoshida M, Hori M, Kamagata K, Suzuki M, et al. Analysis of normal-appearing white matter of multiple sclerosis by tensor-based two-compartment model of water diffusion. Eur Radiol. 2015;25(6):1701-7. Epub 2015/01/13. doi: 10.1007/s00330-014-3572-4. PubMed PMID: 25577520; PubMed Central PMCID: PMCPMC4419192.
10. Temel S, Keklikoglu HD, Vural G, Deniz O, Ercan K. Diffusion tensor magnetic resonance imaging in patients with multiple sclerosis and its relationship with disability. Neuroradiol J. 2013;26(1):3-17. Epub 2013/07/19. PubMed PMID: 23859160.
11. Gratsias G, Kapsalaki E, Kogia S, Dardiotis E, Tsimourtou V, Lavdas E, et al. A quantitative evaluation of damage in normal appearing white matter in patients with multiple sclerosis using diffusion tensor MR imaging at 3 T. Acta Neurol Belg. 2015;115(2):111-6. Epub 2014/07/31. doi: 10.1007/s13760-014-0338-3. PubMed PMID: 25073775.
12. White NS, Leergaard TB, D'Arceuil H, Bjaalie JG, Dale AM. Probing tissue microstructure with restriction spectrum imaging: Histological and theoretical validation. Hum Brain Mapp. 2013;34(2):327-46. Epub 2012/11/22. doi: 10.1002/hbm.21454. PubMed PMID: 23169482; PubMed Central PMCID: PMCPMC3538903.
13. White NS, McDonald C, Farid N, Kuperman J, Karow D, Schenker-Ahmed NM, et al. Diffusion-weighted imaging in cancer: physical foundations and applications of restriction

spectrum imaging. Cancer Res. 2014;74(17):4638-52. Epub 2014/09/04. doi: 10.1158/0008-5472.can-13-3534. PubMed PMID: 25183788; PubMed Central PMCID: PMCPMC4155409.
14. White NS, McDonald CR, Farid N, Kuperman JM, Kesari S, Dale AM. Improved conspicuity and delineation of high-grade primary and metastatic brain tumors using "restriction spectrum imaging": quantitative comparison with high B-value DWI and ADC. AJNR Am J Neuroradiol. 2013;34(5):958-64, s1. Epub 2012/11/10. doi: 10.3174/ajnr.A3327. PubMed PMID: 23139079; PubMed Central PMCID: PMCPMC4146398.
15. McDonald CR, White NS, Farid N, Lai G, Kuperman JM, Bartsch H, et al. Recovery of white matter tracts in regions of peritumoral FLAIR hyperintensity with use of restriction spectrum imaging. AJNR Am J Neuroradiol. 2013;34(6):1157-63. Epub 2013/01/01. doi: 10.3174/ajnr.A3372. PubMed PMID: 23275591; PubMed Central PMCID: PMCPMC3928241.
16. Loi RQ, Leyden KM, Balachandra A, Uttarwar V, Hagler DJ, Jr., Paul BM, et al. Restriction spectrum imaging reveals decreased neurite density in patients with temporal lobe epilepsy. Epilepsia. 2016. Epub 2016/10/14. doi: 10.1111/epi.13570. PubMed PMID: 27735051.
17. McCammack KC, Schenker-Ahmed NM, White NS, Best SR, Marks RM, Heimbigner J, et al. Restriction spectrum imaging improves MRI-based prostate cancer detection. Abdominal radiology (New York). 2016. Epub 2016/02/26. doi: 10.1007/s00261-016-0659-1. PubMed PMID: 26910114.
18. Rakow-Penner RA, White NS, Parsons JK, Choi HW, Liss MA, Kuperman JM, et al. Novel technique for characterizing prostate cancer utilizing MRI restriction spectrum imaging: proof of principle and initial clinical experience with extraprostatic extension. Prostate Cancer Prostatic Dis. 2015;18(1):81-5. Epub 2015/01/07. doi: 10.1038/pcan.2014.50. PubMed PMID: 25559097.
19. Liss MA, White NS, Parsons JK, Schenker-Ahmed NM, Rakow-Penner R, Kuperman JM, et al. MRI-Derived Restriction Spectrum Imaging Cellularity Index is Associated with High Grade Prostate Cancer on Radical Prostatectomy Specimens. Front Oncol. 2015;5:30. Epub 2015/03/06. doi: 10.3389/fonc.2015.00030. PubMed PMID: 25741473; PubMed Central PMCID: PMCPMC4330697.
20. Brunsing RL, Schenker-Ahmed NM, White NS, Parsons JK, Kane C, Kuperman J, et al. Restriction spectrum imaging: An evolving imaging biomarker in prostate MRI. J Magn Reson Imaging. 2016. Epub 2016/08/17. doi: 10.1002/jmri.25419. PubMed PMID: 27527500.

21. Roxburgh RH, Seaman SR, Masterman T, Hensiek AE, Sawcer SJ, Vukusic S, et al. Multiple Sclerosis Severity Score: using disability and disease duration to rate disease severity. Neurology. 2005;64(7):1144-51. Epub 2005/04/13. doi: 10.1212/01.wnl.0000156155.19270.f8. PubMed PMID: 15824338.
22. Droogan AG, Clark CA, Werring DJ, Barker GJ, McDonald WI, Miller DH. Comparison of multiple sclerosis clinical subgroups using navigated spin echo diffusion-weighted imaging. Magn Reson Imaging. 1999;17(5):653-61. Epub 1999/06/18. PubMed PMID: 10372518.
23. Brownlee W, Alves Da Mota P, Prados F, Schneider T, Cardoso MG, Altmann D, et al. Neurite Orientation Dispersion and Density Imaging (NODDI) Is Sensitive to Microstructural Damage Related to Disability in Relapse-Onset MS (S41.003). Neurology. 2016;86(16 Supplement).
24. Schmierer K, Wheeler-Kingshott CA, Boulby PA, Scaravilli F, Altmann DR, Barker GJ, et al. Diffusion tensor imaging of post mortem multiple sclerosis brain. Neuroimage. 2007;35(2):467-77. Epub 2007/01/30. doi: 10.1016/j.neuroimage.2006.12.010. PubMed PMID: 17258908; PubMed Central PMCID: PMCPMC1892244.
25. Stadelmann C, Wegner C, Bruck W. Inflammation, demyelination, and degeneration - recent insights from MS pathology. Biochim Biophys Acta. 2011;1812(2):275-82. Epub 2010/07/20. doi: 10.1016/j.bbadis.2010.07.007. PubMed PMID: 20637864.
26. Shiee N, Bazin PL, Zackowski KM, Farrell SK, Harrison DM, Newsome SD, et al. Revisiting brain atrophy and its relationship to disability in multiple sclerosis. PLoS One. 2012;7(5):e37049. Epub 2012/05/23. doi: 10.1371/journal.pone.0037049. PubMed PMID: 22615886; PubMed Central PMCID: PMCPMC3352847.
27. Mammi S, Filippi M, Martinelli V, Campi A, Colombo B, Scotti G, et al. Correlation between brain MRI lesion volume and disability in patients with multiple sclerosis. Acta Neurol Scand. 1996;94(2):93-6. Epub 1996/08/01. PubMed PMID: 8891052.
28. Nygaard GO, Walhovd KB, Sowa P, Chepkoech JL, Bjornerud A, Due-Tonnessen P, et al. Cortical thickness and surface area relate to specific symptoms in early relapsing-remitting multiple sclerosis. Mult Scler. 2015;21(4):402-14. Epub 2014/08/21. doi: 10.1177/1352458514543811. PubMed PMID: 25139946.